Sara Isabel Rodrigues Azenha
Licenciatura em Biologia

In vivo lineage tracing in lymphopoiesis

Dissertação para obtenção do Grau de Mestre em
Genética Molecular e Biomedicina

Orientador: Drª Vera Sofia Correia Martins
Investigadora Principal, Instituto Gulbenkian de Ciência

Co-orientador: Drª Paula Alexandra Quintela Videira
Investigadora Principal, UCIBIO

Júri:

Presidente: Drª Margarida Castro-Caldas Braga

Arguente: Drª Maria Margarida Teles Vasconcelos Correia Neves

Dezembro, 2020

FACULDADE DE CIÊNCIAS E TECNOLOGIA
UNIVERSIDADE NOVA DE LISBOA

Sara Isabel Rodrigues Azenha
Licenciatura em Biologia

In vivo lineage tracing in lymphopoiesis

Dissertação para obtenção do Grau de Mestre em
Genética Molecular e Biomedicina

Orientador: Drª Vera Sofia Correia Martins
Investigadora Principal, Instituto Gulbenkian de Ciência

Co-orientador: Drª Paula Alexandra Quintela Videira
Investigadora Principal, UCIBIO

Júri:

Presidente: Drª Margarida Castro-Caldas Braga

Arguente: Drª Maria Margarida Teles Vasconcelos Correia Neves

Dezembro, 2020

FACULDADE DE CIÊNCIAS E TECNOLOGIA
UNIVERSIDADE NOVA DE LISBOA

***In vivo* lineage tracing in lymphopoiesis**

Acknowledgments
I would like to offer my special thanks to Dr. Vera Martins for providing guidance and feedback throughout this dissertation and most of all, for receiving me in her lab and giving me the opportunity to work with something I'm so passionate about.

I would like to express my very great appreciation to Dr. Paula Videira for all her support and time spent during this year and for always being interested in my MSc progression.

I am particularly grateful to all my lab members for the patience to teach me all the methodologies and for the tireless hours of explanations. Especially, I would like to thank Camila or "Mother Camila" for always being willing to help solving her "beastie's" problems. Also, Camila and Rafael whose conversations were critical for me to think outside of the box to form an objective point of view and that helped me keep my mental sanity while in the lab during the quarantine. Moreover, I would like to thank Marta and Diogo for the companionship in late-night working. I would like to express my great gratitude to Marta Nogueira whom I grew so fond of, for all the fun times and support.

I would like to extend my many thanks to my family, that made all of this happen and for supporting, motivating, and encouraging me to pursue all my dreams.

Furthermore, I would like to thank my "Serrim" friends, the family I chose, that despite being distant, were always there for me and that never missed the opportunity to make me smile even when things got harder. Most of all, I would like to thank Telma Figueiredo who is my unconditional shelter and the most supportive person in my life. I owe a special thanks to João Gonçalves for all the love and amazing geek conversations but most of all, for believing in me and for motivating me throughout this year. Additionally, I would like to thank my roommates, Laura Meneses and Laura Leirião for putting up with my outbursts and for always being willing to listen and help me through rough times.

Finally, I would like to express one's thanks to all the amazing people in my life that one way or another contributed to my academic career over the years.

Resumo

Os linfócitos diferenciam-se a partir de progenitores hematopoiéticos com origem na medula óssea, onde podem permanecer para originar linfócitos B, ou emigrar e colonizar o timo onde geram os linfócitos T. A existência de progenitores comuns às linhagens de linfócitos B e T foi comprovada experimentalmente com a identificação dos designados *common lymphoid progenitors (CLP)*. No entanto, apesar de as CLP apresentarem uma clara relação de progenitor de linfócitos B, esta mesma relação tem sido amplamente questionada no caso dos linfócitos T, uma vez que que as CLP nunca foram encontradas no timo. Neste contexto, diferentes progenitores foram propostos como sendo o progenitor da linhagem de linfócitos T, mas a sua identidade permanece desconhecida. Esta dissertação aborda esta questão através de *lineage tracing in vivo.* Com o intuito de identificar o progenitor na medula óssea que origina os linfócitos T, analisámos duas linhas de ratinhos: *IL-7rα^{iCre} Rosa26-YFP* e *IL-7rα^{iCre} Rosa26-tdTomato.* Nestes ratinhos, a expressão da Cre segue o padrão de expressão do gene para o *recetor da interleucina 7* (*IL-7rα).* Isto significa que o reporter é expresso e marca células que expressam IL-7rα, assim como a sua descendência. Com tais ferramentas, determinámos relações progenitor-descendência em linhagens linfoides. Adicionalmente usámos um modelo induzível, *IL-7r$\alpha^{iCreERT2}$ Rosa26-tdTomato,* de forma a clarificar essas relações através de análise das populações em diversos momentos após indução do reporter. Identificámos uma população que aparenta ser o progenitor na medula óssea que é homólogo do progenitor mais prematuro no timo. Esta observação foi confirmada em experiências de transferência das células purificadas para recipientes imunodeficientes. Em suma, os nossos dados suportam a noção de que as CLP são uma população heterogénea e nós encontrámos uma subpopulação dentro das CLP que corresponde ao progenitor da medula óssea que origina a linhagem de linfócitos T.

Palavras Chave: Linfócitos, Progenitors Hematopoiéticos, Common Lymphoid Progenitor, Timo

Abstract

Lymphocytes are thought to differentiate from a common progenitor, which either remains in the bone marrow to generate B lymphocytes, or emigrates and, via blood, seeds the thymus to generate T lymphocytes. Such progenitors were originally termed common lymphoid progenitors (CLP), and a bone marrow population with both B and T lymphocyte potential was identified. Although CLP are clearly on their way to feed into the B lymphocyte lineage, their link to the T lymphocyte lineage in physiology is less clear. One concern is that CLP were never found in the thymus. Work from different labs have proposed several bone marrow progenitors as the true progenitors of T lymphocytes, but the identity of such cells remains elusive. Here, we sought to address this aspect by *in vivo* lineage tracing. For that purpose, we analyzed two mouse lines that expressed Cre recombinase from the *interleukin 7 receptor alpha* (*IL-7rα*) endogenous locus that differed in fluorescent reporter: *IL-7rα^{iCre} Rosa26-YFP* and *IL-7rα^{iCre} Rosa26-tdTomato.* In these mice, Cre expression follows the expression pattern of IL-7rα, meaning that it will switch on the reporter to mark IL-7rα expressing cells, as well as all their progeny. With such tools in hand, we could determine progenitor-progeny relationships in the lymphocyte lineages. In addition, we used an inducible model, *IL-7rα^{iCreERT2} Rosa26-tdTomato*, to fine-tune those relationships at several timepoints after reporter induction. We identified a population that seems to be the bone marrow progenitor counterpart of the earliest thymic progenitor. This was validated in adoptive transfer experiments of purified cells into *IL-7rα* deficient recipients. Taken together, our data supports the notion that the CLP is a highly heterogeneous population, and we found a subpopulation within the CLP that is the bone marrow progenitor that originates the T lymphocyte lineage.

Keywords: Lymphocytes, Hematopoietic Progenitors, Common Lymphoid Progenitor, Thymus

Index

Figure Index

Abbreviations

ALP: All-lymphoid progenitor

BCR: B cell receptor

BLP: B-cell-biased lymphoid progenitor

CLP: Common lymphoid progenitor

CMP: Common myeloid progenitor

DC: Dendritic cell

DN: Double negative

DP: Double positive

ERT2: Tamoxifen-inducible estrogen receptor

ETP: Early T cell precursor

FACS: Fluorescent-activated cell sorting

FBS: Fetal bovine serum

GMP: Granulocyte/macrophage progenitor

HSC: Hematopoietic stem cell

i.p.: intraperitoneal

i.v.: intravenous

iCre: improved Cre

IgG: Immunoglobulin G

IL-7r: Interleukin-7 receptor

IL-7rα: Interleukin-7 receptor α chain

Lin: Lineage

LMPP: Lymphoid-primed multipotent progenitor

LoxP: Locus of crossover in P1

LSK: Lineage-negative, Sca1-positive, Kit-positive

MEP: Megakaryocyte/erythrocyte progenitor

MHC: Major histocompability complex

MPP: Multipotent progenitor

NK: Natural killer

NKT: Natural killer T

PBS: Phosphate buffered saline

Rag: Recombination activation gene

SP: Single positive

TCR: T cell receptor

TCRα: T cell receptor α chain

TCRβ: T cell receptor β chain

tdTomato: tandem dimer tomato

TSP: Thymus settling progenitor

V(D)J: Variable Diversity Joining

YFP: Yellow fluorescent protein

1. Introduction

1.1. The immune system

The immune system is composed of all cells and molecules that protect the organism from invading pathogen agents and the damage they cause when the body's barriers are transposed, and eliminate cancer and damaged cells (1). The immune system is classically classified in two main branches: the innate immune system and the adaptive immune system.

1.2. Innate and adaptive immune systems

The innate immune system is the first line of defense of the organism against foreign, potentially pathogenic agents, comprising effectors that are in place to act quickly upon trigger (2). If the physical barriers, i.e. the skin and mucosa that line body cavities, are broken, then pathogens are free to invade the organism. If that happens, then the cells of the innate immune system are recruited to fight and eliminate the threat. These comprehend phagocytes (neutrophils, macrophages, dendritic cells (DC)) and natural killer (NK) cells. These cells express germline encoded receptors that recognize general patterns termed pattern recognition receptors (PRRs) and include the nucleotide oligomerization domain (NOD)-like receptors (NLRs) and toll-like receptors (TLRs). Their ligands are pathogen-associated molecular patterns (PAMPs), that are structural components of microorganisms, and damage-associated molecular patterns (DAMPs), that are products of damaged tissue (3). In response to stimulus, phagocytic cells produce antimicrobial peptides such and phospholipase A2 and Lactoferrin and clear the treat by phagocytosis.

The adaptive immune system is composed of cells bearing cell surface receptors that are encoded by somatically rearranged gene loci. Therefore, these are the only somatic cells that have a unique genome and each express one specific receptor. This characteristic renders them capable of reacting specifically to a given antigen (1). This differs dramatically from the responses mediated by the innate immune system, which recognize general patterns common to several pathogens. However, such characteristic implies that the number of effector cells capable of recognizing a given pathogen is reduced, and therefore the adaptive immune response takes longer to mount. This time is required to expand the responding cells to reach sufficient numbers to effectively clear the infection. The cells of the adaptive immune system are termed lymphocytes, and they can either belong to the T lymphocyte lineage, that differentiates in the thymus, or to the B lymphocyte lineage, that differentiates in the bone marrow and maturate in the spleen. Because every lymphocyte expresses one specific receptor and T and B lymphocytes exist in high numbers altogether, their repertoire is capable of virtually recognizing any given antigen. Antigens are what one terms the molecular structures that are recognized by lymphocyte receptors and one pathogen is typically composed of several antigens (1). Finally, an important feature of the adaptive immune system is memory: after an infection has been cleared the organism retains the memory of that encounter, and that enables a faster and more effective immune response if the same pathogen is encountered again (4).

While one tends to consider the innate and the adaptive immune systems in separate, in reality they work together to clear pathogens and their toxins. Importantly, dendritic cells that belong to the innate immune system present antigens to lymphocytes, thereby stimulating and activating the latter (1).

1.3. Immune response

The immune response constitutes the reaction of the immune system to pathogen exposure or internal trigger (cell damage or carcinogenesis). The earliest steps in the immune response involve the activation of the innate immune system. Interaction between the pattern recognition receptors on effector cells and their ligands triggers a cascade of intracellular signaling events, activating pathways that culminate in the secretion of proinflammatory cytokines and chemokines. These are recognized by several immune cells that are recruited to the place of infection. Macrophages become activated and can eliminate pathogens by phagocytosis, and cells like natural killer (NK) cells can induce death of their target cells (4). Activated dendritic cells present the foreign antigens to lymphocytes, thereby activating them. This happens upon dendritic cell migration into secondary lymphoid organs. The successful interaction of pathogen with antigen-specific lymphocytes results in a response that comprehends the production of antigen-specific antibodies by B lymphocytes, and the expansion and maturation of helper (cytokine producer) or effector (killer) T cells (1). Most protection is mediated by the innate immune system: we seldom realize that we have been exposed to invading bacteria, fungi or viruses. Nevertheless, the adaptive immune response confers an effective and necessary second layer of protection that culminates not only with the successful elimination of the pathogen, but with the organism retaining memory of such encounter.

1.4. Hematopoiesis

All hematopoietic cells, including the cells of the immune system, are generated via a process termed hematopoiesis (Fig. 1.1.). Hematopoiesis is maintained by hematopoietic stem cells (HSC) that in the adult reside in the bone marrow (4). Hematopoietic stem cells self-renew and differentiate into progressively more mature progenitors with restricted differentiation potential, which then give rise to leukocytes, erythrocytes and platelets (1). The first lineage decision is considered to determine the split between the myeloid and the lymphoid lineages, with the emergence of the common myeloid progenitor (CMP) and the common lymphoid progenitor (CLP). The first generates the myeloid cells, thereby sustaining the innate immune system. The latter generates the lymphocytes and thereby sustains mostly the adaptive immune system. Nevertheless, dendritic cells are thought to be an exception since they can originate both from lymphoid and from myeloid lineages, and form a rather heterogeneous population (5).

The common myeloid progenitor differentiates into granulocyte/macrophage progenitors (GMP) or megakaryocyte/erythrocyte progenitors (MEP) (Fig. 1.1.). As their names indicates, GMP differentiate into granulocytes (neutrophils, eosinophils) and monocytes, the latter generating macrophages, and MEP differentiate into erythrocytes and platelets (1).

The common lymphoid progenitor (CLP) has been proposed to generate T and B lymphocytes (Fig. 1.1.). CLP also give rise to the innate lymphoid cells (ILC), that include the natural killer cells which are lymphocytes of the innate immune system. However, the identity of the lymphoid progenitor that under physiological conditions leaves the bone marrow to seed the thymus remains a matter of debate as the CLP was never found in the thymus (6). This will be a topic of discussion in chapter 1.11.

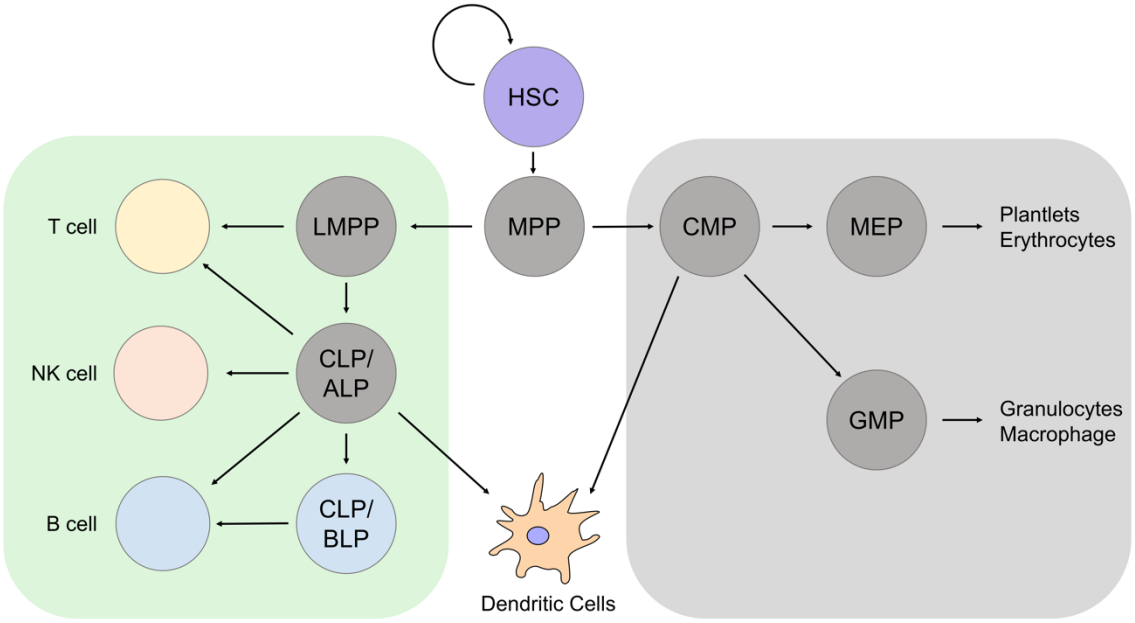

Figure 1.1. Simplified representation of hematopoiesis. All blood cells, including cells of the immune system, originate in self-renewing pluripotent hematopoietic stem cells (HSC). These differentiate into multipotent progenitors (MPP) which in turn give rise to common lymphoid progenitors (CLP) and common myeloid progenitors (CMP). CLP give rise to lymphoid lineages. It is noteworthy that although common lymphoid progenitors give rise to cells of the adaptive immune system (T and B lymphocytes), they also give rise to natural killer (NK) cells which belong to the innate immune system. CMP give rise to granulocyte/macrophage progenitors (GMP) and megakaryocyte/erythrocyte progenitors (MEP). GMP differentiate into granulocytes - neutrophils, eosinophils and basophils – and monocytes, which in turn generate macrophages in specific tissues. MEP differentiate into erythrocytes and platelets. Dendritic cells (DC) can be originated by both CLP and CMP and develop into mature antigen presenting dendritic cells.

1.5. Cells of the adaptive immune system – B lymphocytes

The adaptive immune system is composed by B and T lymphocytes that differentiate in the bone marrow and thymus, respectively, in both mice and humans.

B lymphocytes, or B cells, are continuously produced throughout the life of humans and mice, first in the fetal liver, and then in the bone marrow, after birth (1). The proteins expressed by B lymphocytes for antigen recognition are termed immunoglobulins, and they can be expressed in two forms: membrane bound or secreted. When immunoglobulins are expressed at the surface of the B lymphocytes, they form the B cell receptor (BCR), and their secreted forms are termed antibodies. The immunoglobulins are heterodimeric molecules composed of two identical heavy (H) and two identical light (L) chains (Fig. 1.2.). The immunoglobulin heavy chain is the first to be assembled during B lymphocyte development,

followed by assemble of the light chain. Each chain has a variable (V) and a constant (C) region, and the variable region is the one responsible for antigen recognition. Different constant regions of the immunoglobulins are responsible for different immunoglobulin forms called isotypes, each specialized for activating different effectors (1). In addition to the heavy and light chains, the B cell receptor complex is also composed of Igα and Igβ signaling molecules that are essential for BCR signaling (Fig. 1.2.) (7,8).

B lymphocytes can be activated directly by interaction with an antigen or indirectly through the interaction with helper T cells. B lymphocyte activation results from the recognition of specific antigen by the B cell receptor and leads to the production of antibodies by terminally differentiated B lymphocytes (plasma cells). Antibodies bind antigens, neutralize them, and this enables antigen clearance by other effector cells (1).

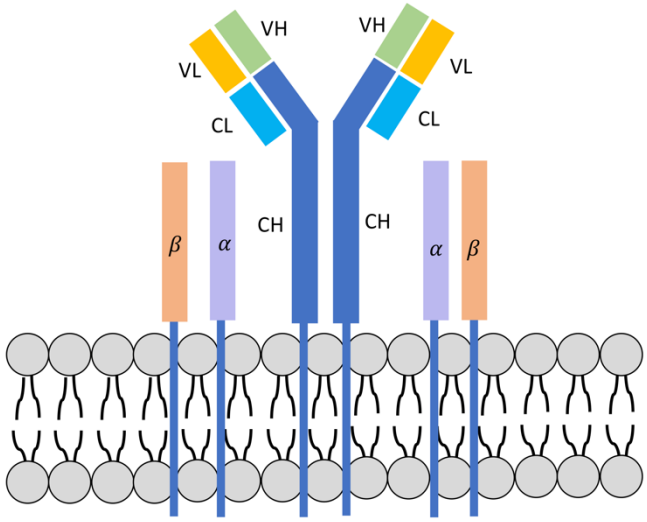

Figure 1.2. B cell receptor (BCR). The B cell receptor is composed by the membrane bound immunoglobulin (mIg) that binds the antigen and a signaling component - an Igα/β heterodimer non-covalently associated with the heavy chains of the mIg. The mIg is a tetramer composed by two heavy (H) chains with a variable (VH) and a constant (CH) region and two light (L) chains, also with a variable (VL) and constant regions (CL).

1.6. Cells of the adaptive immune system – T lymphocytes

In T lymphocytes, or T cells, antigen recognition molecules are always membrane bound and are termed T cell receptors (TCR). T lymphocytes differentiate in the thymus, from hematopoietic progenitors of bone marrow origin. There are two main classes of T lymphocytes, αβ and γδ, which differ in the type of TCR type: αβTCR and γδTCR. Although the chains of each type of TCR differ because they are encoded by different loci, their structure is very similar. Here we focus exclusively on the most prevalent αβ T lymphocytes. The two chains of the αβTCR are encoded by two different genetic loci (α and β) that akin immunoglobulin genes also undergo somatic recombination. TCRα and TCRβ are transmembrane proteins with a variable region, which is responsible for the specific recognition of the antigens and a

constant region (Fig. 1.3.). Each TCR is composed by invariant CD3 chains that are required for TCR signaling: CD3ε, CD3δ, CD3γ and CD3ξ (1).

T lymphocytes can be subdivided based on their functional properties and can be broadly classified as cytotoxic or helper T cells. Cytotoxic T cells express CD8 surface coreceptors and helper T cells express CD4. While CD8 cytotoxic T cells secrete cytokines and kill target cells directly, CD4 helper T cells secrete cytokines and other molecules to help recruiting and potentiate the effector function of other immune cells (1).

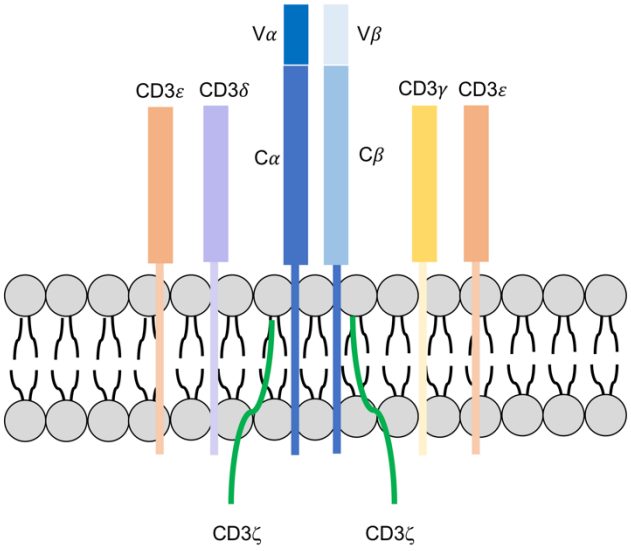

Figure 1.3. T cell receptor (TCR). The αβT cell receptor (αβTCR) is composed by an α chain and a β chain and comprises a variable Vα and Vβ and a constant Cα and Cβ region. Moreover, invariant CD3 (ε, δ, γ, ζ) chains also associate to the TCR and act as a signaling component. γδTCR in γδT lymphocytes have a similar structure.

1.7. Antigen recognition and antigen receptors

A main difference between T and B lymphocytes is how their antigen receptors recognize antigens. While B lymphocytes are able to recognize the antigen directly, T lymphocytes always require antigens to be processed and presented by antigen presenting cells (1). Antigen presenting cells process antigens into short peptides that are presented on the cell's surface by major histocompatibility complex (MHC) molecules. MHC molecules are transmembrane glycoproteins, that are divided in 2 major classes: MHC class I (MHC-I) and MHC class II (MHC-II), which are recognized by cytotoxic T or helper T cells, respectively. Also, the source of peptides presented by MHC-I or MHC-II differ (9). MHC-I can be found in almost every cell and present endogenous and/or intracellular antigens. MHC-II is restricted to antigen presenting cells and presents exogenous and/or extracellular peptides (10). Although T and B lymphocytes recognize antigens differently, their receptors have similar structures. Both receptors have variable regions capable of recognizing specific antigens. In B lymphocytes these are the heavy chain variable regions (VH) and light chain variable regions (VL) (Fig. 1.2.). In T cell receptors, these

variable regions correspond to Vα and Vβ (Fig. 1.3). Variable regions are encoded by different segments which are not contiguous in the genome and need to undergo recombination to produce a complete variable region (Fig. 1.4.) (4). These segments are termed Variable (V), Diversity (D) and Joining (J) segments and their random recombination occurs during the differentiation of T and B lymphocytes. Each rearranged locus will be composed of the one V one D and one J, juxtaposed to encode one functional chain. Therefore, the possible combinations are immense for each chain.

Random recombination of the *TCR* and *Immunoglobulins* loci is mediated by the recombinase complex. This is formed by two proteins that are encoded by the *Recombination activating gene (Rag) 1 (Rag1)* and 2 (*Rag2)*. Rag binds and cleaves DNA at conserved, specific recombination signal sequences that flank each segment. Afterwards, DNA ends are repaired by a set of DNA repair enzymes mainly through non-homologous end joining repair. The cut and paste mediated by Rag is not exact, meaning that the DNA is cut in slightly different locations in each of the gene segments. Further, this process occurs at the same time that the enzyme terminal deoxynucleotidyl transferase (TdT) adds nucleotides randomly to the cut segments. The lack of precision involved increases the diversity generated during somatic recombination of the antigen receptors. Finally, each antigen receptor is formed by 2 types of chains: TCRα and TCRβ in T lymphocytes or heavy and light chains for B lymphocytes. This combinatorial combination increases even further the number of possible receptors each expressed by a given lymphocyte that is unique. It is the whole repertoire composed of all lymphocytes that ensures the recognition of any given antigen.

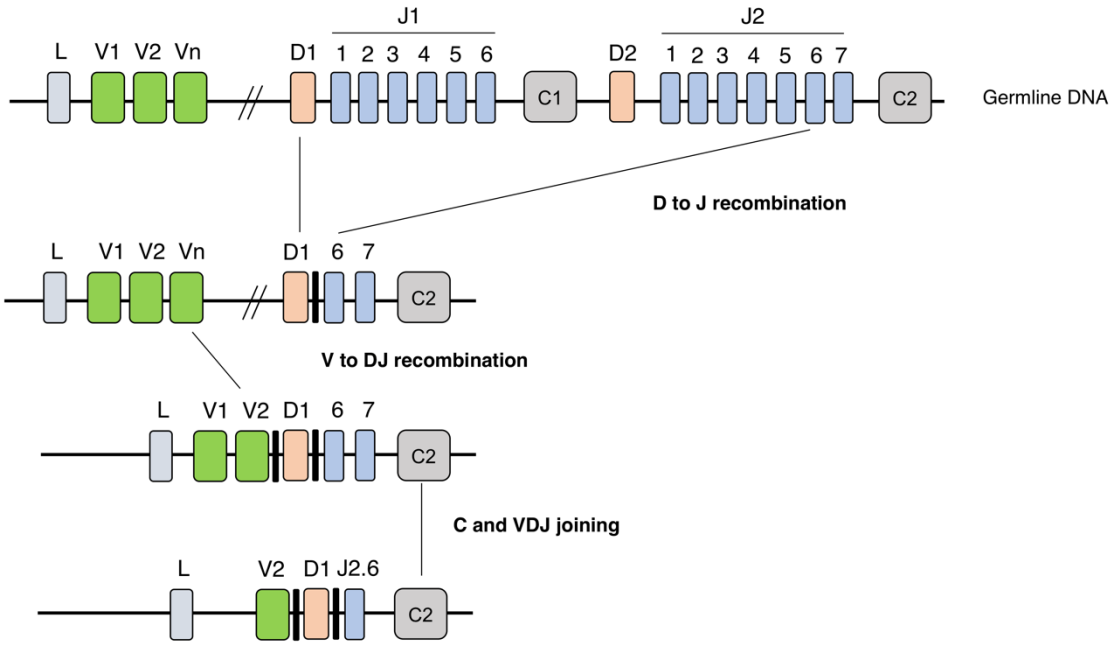

Figure 1.4. Variable region rearrangement. Schematic representation of the *TCRβ* locus. During recombination mediated by Rag activity, the locus undergoes changes in the genomic DNA. First, a Diverse (Dβ) segment is joined with a Joining (Jβ) segment. Following, a Variable (Vβ) segment is recombined with the DβJβ region. The rearranged VβDβJβ region is then joined to a constant (C) region.

1.8. Lymphopoiesis and lymphoid organs

Lymphopoiesis or lymphocyte differentiation takes place in the primary lymphoid organs: the fetal liver (during embryonic development), the bone marrow and the thymus. In these specialized lymphoid tissues, stromal cells provide the adequate microenvironments that support lymphocyte differentiation. While all hematopoietic progenitors originate in the bone marrow, this is also the main site of B lymphocyte differentiation. In contrast, T lymphocytes differentiate in the thymus from hematopoietic progenitors that must leave the bone marrow and seed the thymus (1). The lymphoid organs where adaptive immune responses take place are termed secondary lymphoid organs and include the spleen and lymph nodes. These are the organs where some immune cells, like B lymphocytes, complete differentiation (1).

1.9. B lymphocyte differentiation

B lymphocyte differentiation (Fig. 1.5.) starts in the bone marrow and terminates in the spleen. It comprises an antigen independent phase preceding an antigen dependent phase.

Common lymphoid progenitors (CLP) express the Ikaros transcription factor which leads to up-regulation of *Ebf1* and *Pax5,* the latter driving B cell commitment (11,12). The commitment to the B lymphocyte lineage, as well as proliferation and survival of several populations of B cell committed precursors, depends on interleukin-7 (IL-7) that is produced by bone marrow stromal cells (13,14). B lymphocyte commitment *per se* occurs at the pre-proB stage, or fraction A (12,15). These cells express B220 and CD43, but not the pan-B cell marker CD19 ($B220^+$, $CD43^+$, $CD19^-$) (16–18), which only starts at the next stage, the proB cells, or fraction B (18). In proB stage of differentiation ($B220^+$, $CD43^+$, $CD24^+$, $CD19^+$), expression of both E2A and EBF1 transcription factors induce expression of the genes *Rag1* and *Rag2*, thereby initiating recombination of the heavy chain locus of the B cell receptor (BCR) (1). At this stage, two invariant “surrogate” proteins resembling the light chain are produced and pair with the heavy chain, forming the pre-B cell receptor (pre-BCR). Signaling from the pre-BCR triggers the expression of the IL-7 receptor (IL-7r), and therefore renders proB cells sensitive to IL-7, thus upregulating anti-apoptotic factors. Therefore, all cells that fail to generate a heavy chain are eliminated. ProB cells then differentiate into early preB stage, or fraction C ($B220^+$, $CD43^+$, $CD24^{high}$, $CD19^+$). Later, late preB stage cells, or fraction D ($B220^+$, $CD43^-$, $CD19^+$, IgM^-), undergo rearrangement of the light chain locus, which allows cells to progress into immature B cell stage or fraction E ($B220^+$, $CD43^-$, $CD19^+$, IgM^+), with a fully developed naïve BCR (1). Immature B cells then migrate towards secondary lymphoid organs where they undergo maturation, giving rise to mature B cells, or fraction F. Newly formed mature B cells express CD93, while recirculating mature B cells have already downregulated this receptor (18). CD93 is a fetal stem cell marker found in all precursor stages of B lymphocytes (19).

Upon contact with pathogen-derived antigens and with the help of T cells residing in these tissues, naïve mature B cells enter germinal centers where they expand and undergo somatic hypermutation of the antibody-encoding genes, in order to increase the antibody affinity to the pathogen (1,20).

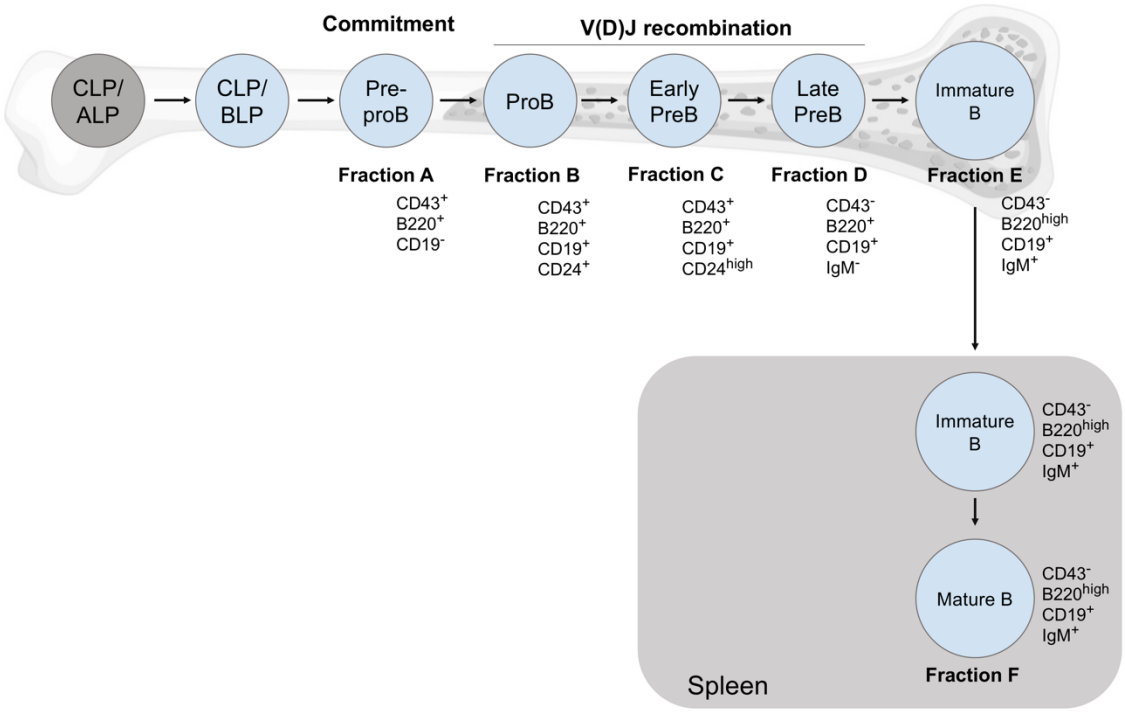

Figure 1.5. B lymphocyte differentiation. B lymphocytes develop in the bone marrow from common lymphoid progenitors (CLP). The first reported stage of B lymphocyte development is the pre-proB stage (Fraction A) ($CD43^+$, $B220^+$, $CD19^-$). Cells undergo subsequent stages of differentiation comprising proB stage (Fraction B) ($CD43^+$, $B220^+$, $CD19^+$, $CD24^+$), early PreB (Fraction C) ($CD43^+$, $B220^+$, $CD19^+$, $CD24^{high}$) and late preB (Fraction D) ($CD43^-$, $B220^+$, $CD19^+$, IgM^-) until they reach the stage of immature B cells (Fraction E) ($CD43^-$, $B220^{high}$, $CD19^+$, IgM^+) expressing a functional yet naïve B cell receptor (BCR). Immature B cells then migrate into secondary lymphoid organs where they maturate into mature B cells (Fraction F) ($CD43^-$, $B220^{high}$, $CD19^+$, IgM^+).

1.10. T lymphocyte differentiation

In the thymus (Fig. 1.6.), $\alpha\beta$ thymocytes can be subdivided based on CD4 and CD8 expression. The most immature thymocytes express neither and are therefore termed double negative (DN) thymocytes. The DN stages can be further subdivided based on the expression of CD44, CD25 and Kit. The most immature stage in the thymus is the early T cell precursor (ETP: $CD44^+$, $CD25^-$, Kit^+), which differentiate progressively into DN2a ($CD25^+$, $CD44^+$, Kit^+), DN2b ($CD25^+$, $CD44^+$, Kit^{int}), DN3 ($CD25^+$, $CD44^-$, Kit^-), DN4 ($CD25^-$, $CD44^-$, Kit^-). DN4 quickly differentiate into CD4/CD8 double positive (DP) cells, passing through a transient immature CD8 single positive stage (ISP). DP cells account for ~80% of all thymocytes (21). Finally, double positive thymocytes downregulate CD4 or CD8 to become CD8 or CD4 single positive (SP) thymocytes, that then leave the thymus (1,4).

Differentiation associates with a migration pattern in the thymus that is considered to enable differentiating thymocytes to gain access to important cytokines and growth factors that are specific of each given stage. In this context, hematopoietic progenitors enter the thymus at the corticomedullary junction, where ETP can be found, and then differentiate into DN2 that migrate throughout the cortex

towards the capsule, where DN3 accumulate. Double positive thymocytes occupy the whole cortex, but the single positive thymocytes migrate into the medulla (22).

T lymphocyte differentiation depends on the rearrangement of the *TCR* genes, and selection steps that test for TCR functionality. The first step is *TCRβ* recombination (Fig. 1.4.) that starts at DN2 and continues through DN3 stage. Successfully rearrangement of productive (in-frame) *TCRβ* will lead to protein expression and β-selection (23). Specifically, the TCRβ pair with the surrogate pre-T cell receptor α (pre-TCRα) chain to form the pre-TCR complex which give thymocytes a survival signal that rescues them from apoptosis and induces proliferation. β-selection tests for successful rearrangement of the *TCRβ* locus, and proliferation expands the pool of thymocytes with a productive *TCRβ* locus. After, double positive thymocytes recombine their *TCRα* locus. TCRα depends only on one step of Vα-Jα recombination. Upon TCR expression, thymocytes are tested for the functionality of the receptor. Because TCR are generated through a random mechanism of gene rearrangement, it is possible that the receptors are non-functional or that recognize self-molecules. Both types of receptors are indeed generated, but those cells die in the thymus resulting from positive and negative selection. Until the double positive stage, T lymphocyte development is independent of MHC molecules. Double-positive thymocytes that can recognize self-peptides:MHC complexes with low affinity receive a survival signal and differentiate further into CD4 or CD8 single positive thymocytes. The CD4/CD8 lineage specification is also dependent on TCR-MHC interactions. DP thymocytes for which the TCR interacts strongly with MHC class I molecules will commit to the CD8 T (cytotoxic) cell lineage, while DP cells containing a TCR that interacts with MHC class II molecules downregulate CD8 and differentiate into CD4 (helper) T cells. Single positive thymocytes migrate into the medulla, where they undergo negative selection. Specifically, thymocytes expressing TCR that recognizes self-peptides presented by MHC complexes too vigorously are eliminated, ensuring that only self-tolerant mature naive T lymphocytes are exported to the periphery (1). Some CD4 thymocytes enter and alternative lineage: the regulatory T cells (Tregs), which express Foxp3 transcription factor, and suppress immune function to control immune responses and prevent autoimmunity (24).

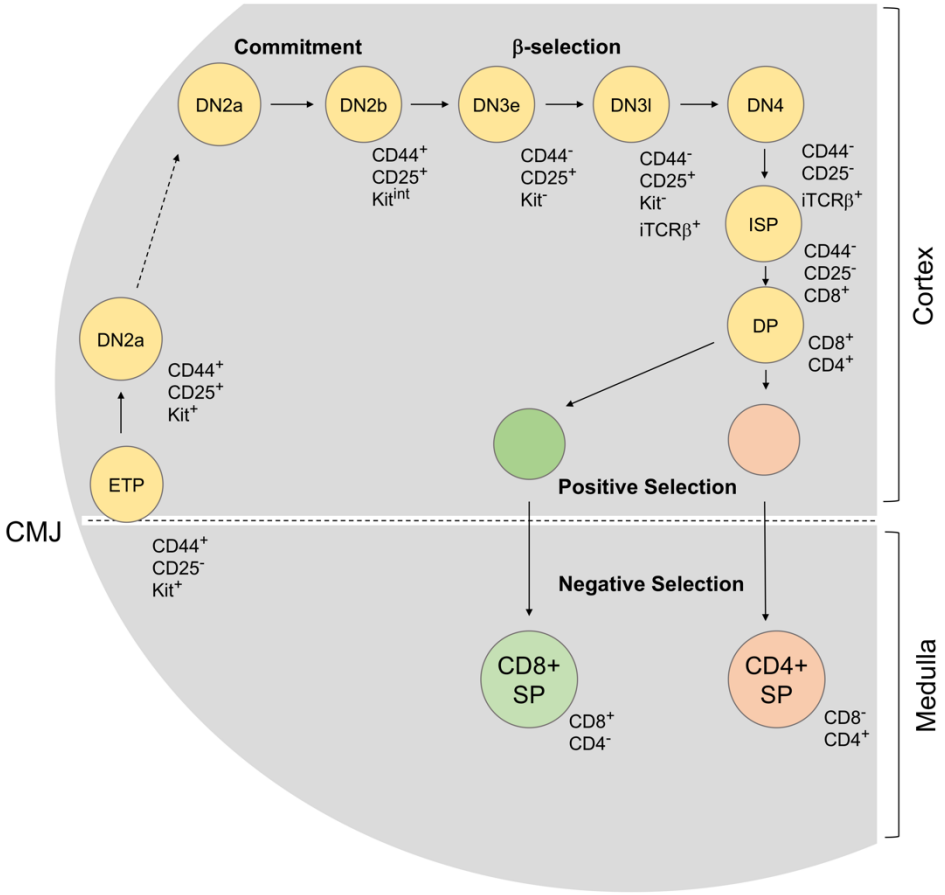

Figure 1.6. T lymphocyte development. The thymus is a primary lymphoid organ organized in two main regions: the cortex and the medulla. Bone marrow progenitors seed the thymus at the corticomedullary junction (CMJ), giving rise to the early T cell precursor (ETP). ETP differentiate successively into double negative (DN) thymocytes DN2a (Kit^+, $CD25^+$, $CD44^+$), DN2b (Kit^{int}, $CD25^+$, $CD44^+$), DN3 (Kit^-, $CD25^+$, $CD44^-$) and DN4 (Kit^-, $CD25^-$, $CD44^-$). DN3 are further subdivided into early DN3 (DN3e) and late DN3 (DN3l) based on the expression of intracellular TCRβ (iTCRβ) and β-selection takes place in between. After DN4 stage, cells undergo a rapid transition through a transient immature CD8 single positive stage (ISP) and enter double positive stage (DP) ($CD8^+$, $CD4^+$). After, cells undergo positive selection in the cortex and negative selection in the medulla and develop into CD4 or CD8 single positive T cells.

1.11. Hematopoietic progenitors seeding the thymus

Common lymphoid progenitors (CLP) were the first identified progenitor proposed to be in the origin of both T and B lymphocyte lineages (25). However, CLP were never found in the thymus (6) and the markers they express do not fully fit those expressed by the most immature T cell progenitor in the thymus, the early T cell precursor (ETP). Therefore, several other bone marrow progenitors that have T cell potential, were proposed as the physiological counterpart of the ETP (26–29). These include the HSC themselves, and the Lymphoid-primed multipotent progenitors (LMPP) (Fig. 1.7.) (30), as well as subsets of CLP and LMPP.

The CLP is a heterogeneous population defined as Flt3-positive, IL-7r-positive (31). Further expression of Ly6D subdivides the CLP into Ly6D-negative all-lymphoid progenitor (ALP), and Ly6D-positive or B-cell-biased lymphoid progenitor (BLP) that are already biased towards B lymphopoiesis (32). Within the LMPP, L-selectin expressing LMPP were described to resemble the ETP and therefore pointed out as the thymus settling progenitor (33). Interestingly, while CLP have been described as lacking myeloid potential (25), LMPP still retain this potential (30), a feature shared with early committed T cell progenitors (ETP), that still retain some B cell and myeloid potential (34).

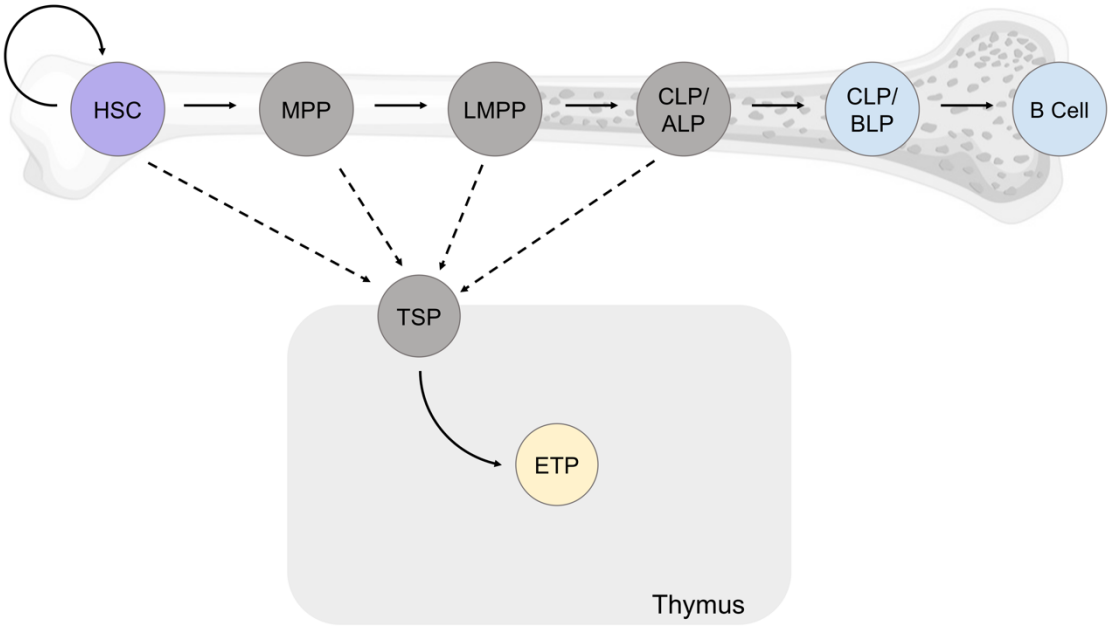

Figure 1.7. Candidate progenitors with T cell potential. Many bone marrow progenitors have been shown to have T cell potential and therefore hypothesized to be able to seed the thymus and give rise to the thymus settling progenitor (TSP) and therefore the early T cell precursor (ETP). Among which are the HSC themselves, the multipotent progenitor (MPP), the lymphoid-primed LMPP and common lymphoid progenitors (CLP), more precisely the subpopulation that lacks expression of Ly6D marker – the All-lymphoid progenitor (ALP). The Ly6D-positive fraction (BLP) of the CLP is thought to be biased towards the B cell lineage.

2. Aims and Objectives

This thesis aimed at elucidating the identity of the bone marrow progenitor that under physiologic conditions emigrate out of the bone marrow and seed the thymus to support T lymphocyte differentiation *in vivo* and in unperturbed hematopoiesis. With that purpose, two novel mouse strains had been generated in the laboratory and crossed to fluorescent reporter mouse lines. The first strain allowed lineage tracing from a constitutively expressed Cre recombinase. The second strain was an inducible Cre recombinase, that recombined the reporter upon tamoxifen injection.

Therefore, the following objectives were proposed:

Objective 1. Characterize reporter expression during lymphopoiesis in *IL-7r$\alpha^{iCre/+}$ Rosa26-YFP* mice

Objective 2. Characterize reporter expression during hematopoiesis in *IL-7r$\alpha^{iCre/+}$ Rosa26-tdTomato* mice

Objective 3. Isolate and perform adoptive transfer of candidate bone marrow progenitors to assess their thymus reconstitution capacity

Objective 4. Characterize the temporal dynamics of reporter expression in inducible *IL-7r$\alpha^{iCre-ERT2/+}$ Rosa26-tdTomato*

3. Materials and Methods

3.1. Mice

B6.SJL-*Ptprc*^{a} *Pepc*^{b}/BoyJ (CD45.1+) (JAX stock #002014, here termed *B6.SJL*), B6.129S7-*Il7r*^{tm1Imx}/J (35) (JAX stock #002295, here termed *IL-7rα*$^{-/-}$), B6.Cg-*Gt(ROSA)26Sor*$^{tm14(CAG-ttdTomato)Hze}$ (36) (JAX stock #007914, here termed *Rosa26-tdTomato*) mice were purchased from The Jackson Laboratory, bred and maintained at the *Instituto Gulbenkian de Ciência (IGC).* B6.129X1-*Gt(ROSA)26Sor*$^{tm1(EYFP)Cos}$/J (37) here termed *Rosa26-YFP* were also bread and kept at the IGC. B6.Cg-*Commd10*$^{Tg(Vav1-icre)A2Kio}$/J (38) (JAX stock #008610, here termed *Tg(Vav-iCre)* mice were purchased from Charles River and crossed with *Rosa26-YFP* or *Rosa26-tdTomato* to obtain *Tg(Vav-iCre) Rosa26-YFP* or *Tg(Vav-iCre) Rosa26-tdTomato* reporter mice, respectively. *Rag2*$^{-/-}$ $\gamma_c^{-/-}$ mice were imported from the University of Ulm, Germany, through embryo rederivation. All mice were analyzed at the age of 4- to 10-weeks. Mice were kept in individually ventilated cages in specific pathogen-free (SPF) conditions and all experimental procedures were performed according to the established national normative for animal experimentation, approved by the Ethics Committee of the IGC – *Fundação Calouste Gulbenkian* and *Direção Geral de Alimentação e Veterinária (DGAV).*

3.2. Generation of the *IL-7rα*^{iCre} and *IL-7rα*^{iCreERT2} mouse models

IL-7rα^{iCre} and *IL-7rα*^{iCreERT2} mouse models were previously generated in our laboratory by introducing the coding sequence for the *codon-improved Cre (iCre)* (39) or for *iCre* fused with a *tamoxifen-inducible estrogen receptor (ERT2)* (40) into the first exon of the endogenous *IL-7rα* locus. The targeting was done using CRISPR-Cas9 technology at the Transgenics Facility of the IGC. *IL-7rα*^{iCre} expresses iCre constitutively from the endogenous *IL-7rα* promotor. In *IL-7rα*^{iCreERT2} mice, iCre-ERT2 is also expressed from the endogenous *IL-7rα* promotor, but the protein is kept inactive in the cytoplasm until activation is induced by tamoxifen administration. Both mouse strains were crossed with *Rosa26-YFP* and *Rosa26-tdTomato* to generate: *IL-7rα*$^{iCre/+}$ *Rosa26-YFP, IL-7rα*$^{iCre/+}$ *Rosa26-tdTomato, IL-7rα*$^{iCreERT2/+}$ *Rosa26-YFP*, and *IL-7rα*$^{iCreERT2/+}$ *Rosa26-tdTomato.*

3.3. Tamoxifen Administration

Tamoxifen (Sigma T5648) was dissolved for a final concentration of 10 mg/mL in corn oil at 55°C (Sigma C8267) with 10% ethanol. Aliquots were then stored at -20°C and pre-heated to 37°C, protected from light, prior to administration. Each mouse (4- to 6-week-old) received 1 mg of tamoxifen (100 μl) via intraperitoneal (i.p.) injection or via gavage. Mice received one single administration for most experiments, or five daily administrations where indicated.

3.4. Sample preparation

Mice were euthanized and organs harvested. Single cell suspensions of thymus and spleen were prepared in PBS/10% FBS by mashing the organs through 40 μm nylon cell strainers. Bone marrow was flushed out of femurs and tibias and single cell suspensions were also passed through 40 μm nylon cell strainers. Live cells were counted in a hemocytometer using Trypan Blue for dead cell exclusion.

3.5. Analysis by flow cytometry

One or two million cells, depending on the staining, were blocked with mouse IgG (112mg/ml, Jackson ImmunoResearch) for 15 minutes. Staining of samples was performed for 30 minutes on ice in the dark using appropriate antibody dilutions. When necessary, a second step staining of 30 minutes was carried out after two washes with PSB/10% FBS. The following antibodies were purchased from Biolegend: B220 (RA3-6B2), CD3ε (145-2C11), CD4 (GK1.5), CD8α (53-6.7), CD11b (M1/70), CD11c (N418), CD19 (6D5), CD24 (M1/69; 30F1), CD25 (PC61), CD43 (S11), CD44 (IM7), CD45.1 (A20), CD45.2 (104), CD49b (DX5), CD62L (MEL-14), CD93 (AA4.1), CD150 (TC15-12F12.2), Kit (2B8), F4/80 (BM8), Flt3 (A2F10), Gr1 (RB6-8C5), IgM (RMM-1), IL-7rα (A7R34), Ly6D (49-H4), NK1.1 (PK136), Ter119 (TER-119), Sca1 (D7), conjugated to the following fluorochromes: FITC, PE, PE-Cy7, PerCP-Cy5.5, APC, APC-Cy7, Biotin, BV711, BV605, BV650, BV421, Pacific Blue. CD4 (GK1.5) APC was produced *in house* by the Antibody Facility. The lineage (Lin) cocktail was composed of CD4, CD8α, CD3ε, CD11b, CD11c, NK1.1, CD19, Gr1 and Ter119 antibodies. For stainings focusing exclusively on B lymphocyte differentiation, the lineage cocktail lacked CD19, Gr1 and Ter119. Streptavidin conjugated to BV785 or APC-Cy7 was used to recognize biotinylated antibodies. Dead cells were excluded with Sytox Blue (Invitrogen) or with Zombie dye in Pacific Orange (Biolegend). Zombie stainings were performed in PBS for 30 minutes at room temperature and preceded by a wash with PBS, as indicated by the supplier. All samples were acquired using a BD LSRFortessa™ X-20 Flow Cytometer (BD Biosciences) and analyzed using FlowJo 10.6.2 (FlowJo LLC, USA).

3.6. Cell sorting and adoptive transfers into *IL-7rα*$^{-/-}$ mice

Single cell suspensions of bone marrow from wild type *B6.SJL* (CD45.1) were blocked with mouse IgG for 15 minutes and stained with the following antibodies: Sca1 (D7) PerCP-Cy5.5, Kit (2B8) APC, IL-7rα (A7R34) PE-Cy7, Flt3 (A2F10) PE, Ly6D (49-H4) FITC and a biotin-conjugated lineage cocktail defined as above. A second step staining with streptavidin APC-Cy7 was performed after two washes. Dead cells were excluded using Sytox Blue (Invitrogen). Cells were first sorted in yield for lineage-negative, Sca1-positive, Kit-positive (LSK) cells, and common lymphoid progenitors (CLP), the latter defined as Lineage-negative, Flt3-positive, IL-7r-positive. Afterwards, LSK were sorted for Flt3-positive (in purity) that define the lymphoid-primed multipotent progenitors (LMPP) and split according to their expression for IL-7rα: IL-7rα-positive LMPP (LMPP IL-7r^{+}) versus IL-7rα-negative LMPP (LMPP IL-7r^{-}). Similarly, CLP were sorted a second time (for purity) and split according to their expression for Ly6D as: Ly6D-negative (CLP Ly6D^{-}) versus Ly6D-positive (CLP Ly6D^{+}). Cells were collected into FBS coated tubes

containing sterile PBS/50% FBS, and purity of the sorted populations was assessed at the end of the sorting. Cell sorts were performed using a BD FACSAria^{TM} II Cell Sorter (BD Biosciences).

Sorted cells were resuspended in sterile PBS containing *Rag2*$^{-/-}$ $\gamma_c^{-/-}$ splenocytes as carrier cells and cell suspensions were injected intravenously (i.v.) in the tail vein of 8-week-old *IL-7r*$\alpha^{-/-}$ recipients (CD45.2). Experimental groups received 1500 LMPP IL-7r^{+} cells, 1500 LMPP IL-7r^{-}, 7865 CLP Ly6D^{+} or 7865 CLP Ly6D^{-}. Each group consisted of two mice. All mice were analyzed 21 days after reconstitution.

3.7. Data analysis and statistical analysis

Flow cytometry data was analyzed with FlowJo 10.6.2 (FlowJo LLC, USA). For statistical analysis and graphic representation of the data GraphPad'sPrism 8.2.1 (GraphPad Software, USA) was used.

4. Results

4.1. *In vivo* lineage tracing in *IL-7rα*$^{iCre/+}$ *Rosa26-YFP* mice

We sought to detail *in vivo* progenitor-progeny relationships between bone marrow, and T lymphocyte precursors. For that purpose, we generated a new mouse model by targeting the *IL-7rα* endogenous locus. The sequence for a *codon improved-Cre (iCre)* recombinase was inserted into the first exon of the *IL-7rα* (Fig. 4.1. A), following a published design (41). Mice were then crossed to the reporter line *Rosa26-YFP*, that expresses yellow fluorescent protein (YFP) upon Cre recombination (37). Specifically, *Rosa26-YFP* mice have a floxed stop cassette that prevents YFP expression from the ubiquitous *Rosa26* locus (Fig. 4.1. A). Upon Cre expression, the stopper cassette is excised, and the reporter gene is expressed (Fig. 4.1. A). In this model, YFP expression will mark all cells that either express IL-7rα, or have a history of IL-7rα expression. Since *IL-7rα*^{iCre} is a knock-in/knockout, we always analyzed heterozygote *IL-7rα*$^{iCre/+}$ mice, that have reduced IL-7rα expression without affecting the hematopoietic system or lymphocyte development, according to former results from other mouse models disrupting the *IL-7rα* locus (35,41).

We characterized adult *IL-7rα* $^{iCre/+}$ *Rosa26-YFP* mice and compared them to negative and positive controls, wild type *B6.SJL* and *Tg(Vav-iCre) Rosa26-YFP*, respectively. *Tg(Vav-iCre) Rosa26-YFP* was chosen because the Cre is expressed from very early in hematopoiesis and therefore all hematopoietic cells are YFP-positive. We started the characterization by analyzing bone marrow progenitors, namely the lineage-negative, Sca1-positive, Kit-positive (LSK) that contains the hematopoietic stem cells and very immature hematopoietic progenitors. In *IL-7rα* $^{iCre/+}$ *Rosa26-YFP* mice, the LSK contained nearly no YFP-positive cells (Fig. 4.1. B). Further gating for LSK Flt3-high to define lymphoid-primed multipotent progenitors (LMPP), we found a minor population that expressed IL-7rα protein, and within that population few cells were YFP-positive, consistent with recombination of the *Rosa26-YFP* locus in that population (Fig. 4.1. B). As expected, the CLP that is defined by IL-7rα expression (25), also expressed the YFP reporter (Fig. 4.1. B).

In the thymus, T lymphocyte differentiation was characterized as shown in Fig. 4.1. C. YFP expression was detected at all stages of differentiation, starting from the most immature early T cell precursor (ETP) (Fig. 4.1. C). The quantification of the reporter expression in each population, starting in the bone marrow progenitors, covering the thymus and the T lymphocytes at the periphery, shows a cumulative increase in the percentage of YFP reporter-positive cells (Fig. 4.1. D). This is consistent with expression of the IL-7rα, and therefore of iCre, at several stages of T lymphocyte differentiation (42). These data validate this mouse model to be further used to determine progenitor-progeny relationships between hematopoietic progenitors in the bone marrow, and their counterparts in the thymus.

Concerning the progenitor-progeny relationships that we were interested to tackle, we focused on the bone marrow progenitors CLP and LMPP. Considering simple lineage tracing principles, if a progenitor population is YFP-positive, its progeny can only be YFP-positive. Further, the percentage of recombined cells must either be the same between progenitor-progeny, if the latter does not express iCre, or higher in the progeny, if the progeny also expresses iCre. The percentage of YFP-positive CLP was significantly higher than that of the ETP, excluding the CLP population from preceding the ETP (Fig. 4.1. D). The other population that has been postulated to be the bone marrow counterpart of the ETP is the LMPP. As a whole, the levels of YFP expression in LMPP are residual. Nevertheless, we checked for YFP expression in two subpopulations: LMPP expressing L-selectin (LMPP CD62L^{+}) and a minor subpopulation that expresses IL-7rα (LMPP IL-7r^{+}). The LMPP CD62L^{+} contained residual levels of YFP-positive cells. Interestingly, the levels of YFP-positive LMPP IL-7r^{+} were very similar, albeit slightly lower, than those of the ETP (Fig. 4.1. D). Altogether, these data exclude the CLP (as a whole population) from being the direct progenitor of the ETP. Furthermore, it points at LMPP IL-7r^{+} as the most likely progenitor population upstream of the ETP.

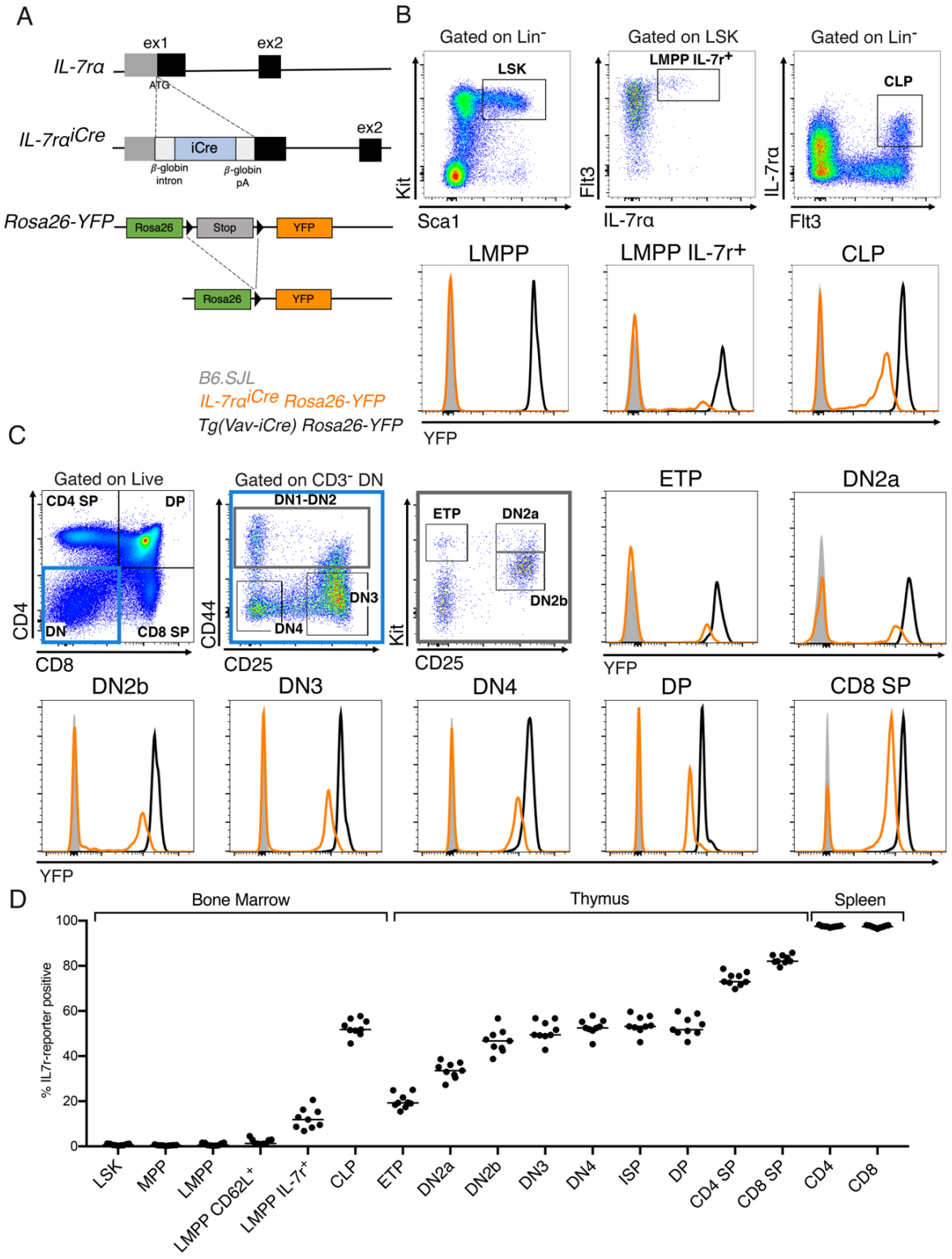

Figure 4.1. *IL-7rα^{iCre} Rosa26-YFP* characterization and T lymphocyte differentiation. A. Schematic representation of the wild type *IL-7rα* locus and the targeted *IL-7rα^{iCre}* allele. The *Rosa26-YFP* locus is represented before and after Cre mediated recombination. **B.** Bone marrow from *IL-7rα^{iCre} Rosa26-YFP* mice was analyzed by flow cytometry for the indicated markers to acess the candidate progenitor populations. Representative FACS plots of *IL-7rα^{iCre} Rosa26-YFP* mice are depicted together with YFP expression in each population in *IL-7rα^{iCre} Rosa26-YFP* mice (orange) compared to a *B6.SJL* (gray filled) and a *Tg(Vav-iCre) Rosa26-YFP* (black) control. **C**. Thymus from *IL-7rα^{iCre} Rosa26-YFP* mice was analyzed by flow cytometry for the indicated markers to access T lymphocyte differentiation stages. Representative FACS plots are depicted together with YFP expression in each thymocyte population in *IL-7rα^{iCre} Rosa26-YFP* mice (orange) compared to a *B6.SJL* (gray filled) and a *Tg(Vav-iCre) Rosa26-YFP* (black) control. **D.** Quantification of the labeling frequencies of bone marrow progenitors and thymocytes. Data corresponds to 3 independent experiments, with n=3 mice in each experiment. Each dot corresponds to one mouse and the bar represents the median.

In addition to T lymphocyte development, we also assessed other cell lineages in *IL-7rα^{iCre} Rosa26-YFP* mice. IL-7 signaling is also important for B lymphocyte differentiation, and the receptor is expressed at several stages during B lymphocyte commitment and development. B lymphocyte differentiation starts in the bone marrow and terminates in the spleen. We focused on the immature stages of B lymphocyte differentiation and found that all stages contained a fraction of YFP-positive cells (Fig. 4.2. A). There was an increase in the percentage of YFP-positive cells from the CLP to the pre-proB, and then to the proB cells (Fig. 4.2. B). Thereafter, all stages expressed the reporter at maximum levels (Fig. 4.2. B). It is interesting that B lymphocytes have higher percentage of YFP reporter-positive cells throughout differentiation as compared to T lymphocyte differentiation. This suggests that B lymphocyte precursors express higher levels of IL-7rα than T lymphocyte precursors. Altogether, these data are in line with the literature, and with CLP being immediately upstream of the first stage of differentiation originating the B lymphocyte lineage.

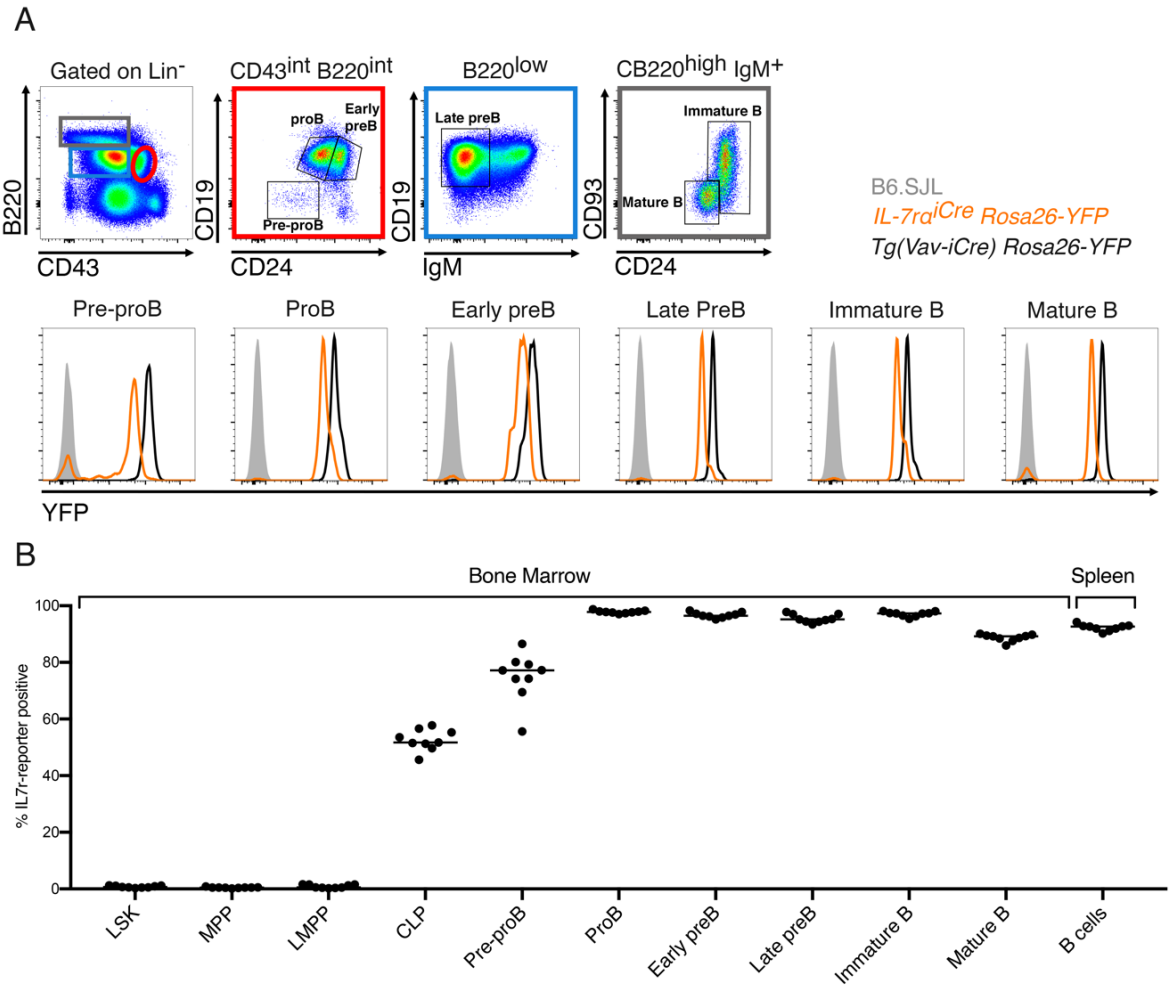

Figure 4.2. *IL-7rα^{iCre} Rosa26-YFP* mice, B lymphocyte differentiation. A. Bone marrow from *IL-7rα^{iCre} Rosa26-YFP* mice was analyzed by flow cytometry for the indicated markers to access B lymphocyte differentiation stages. Representative FACS plots of *IL-7rα^{iCre} Rosa26-YFP* mice are depicted together with YFP expression in each population in *IL-7rα^{iCre} Rosa26-YFP* mice (orange) compared to a *B6.SJL* (gray filled) and a *Tg(Vav-iCre) Rosa26-YFP* (black) control. **B.** Quantification of the labeling frequencies of bone marrow progenitors and stages of B lymphocyte differentiation. Data corresponds to 3 independent experiments, with n=3 mice in each experiment. Each dot corresponds to one mouse and the bar represents the median.

Next, we set to analyze two other lineages, NK and NKT cells. Conventional natural killer (NK) cells develop in the bone marrow and mature in secondary lymphoid organs such as the spleen (43). In addition, one subset has been reported to develop specifically in the thymus - thymic NK cells (44). These cells differ from conventional NK in that they express IL-7r and GATA-3 (44). Likewise, NKT cells also express IL-7rα (45). NKT are a small subset of αβT lymphocytes that also expresses NK1.1. We addressed the levels of YFP expression in these two cell lineages in the thymus (Fig. 4.3. A) and in the spleen (Fig. 4.3. B). Both NK and NKT have a large fraction of YFP-positive cells (Fig. 4.3. C), consistent with their expression of IL-7rα at some stage during differentiation.

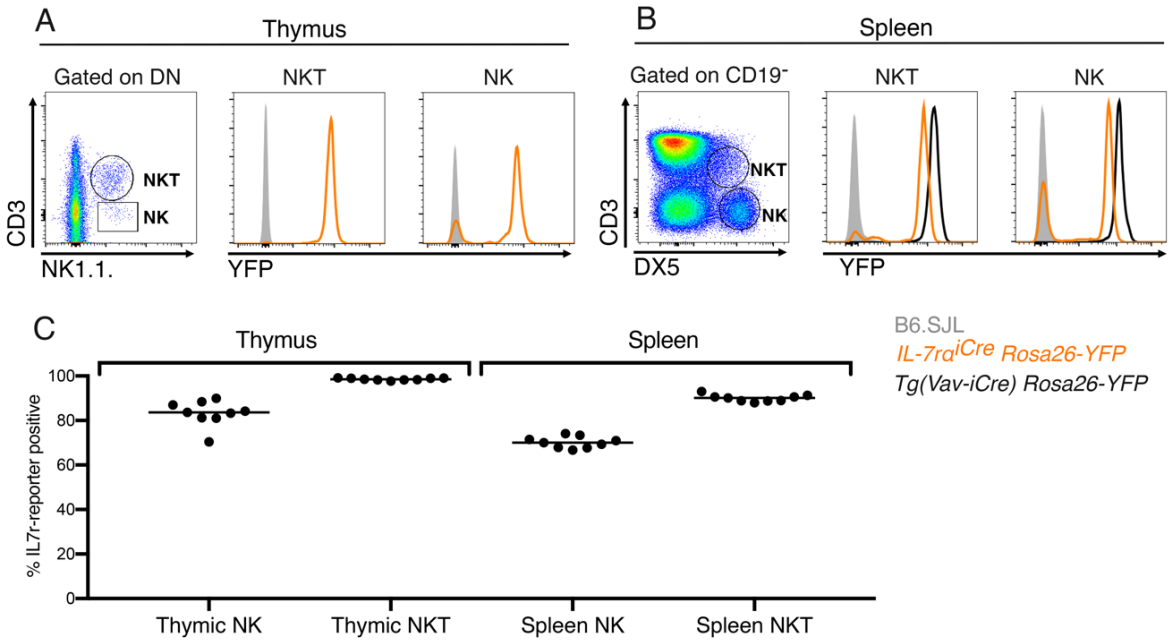

Figure 4.3. *IL-7rα^{iCre} Rosa26-YFP* mice, natural killer cells. A. Thymus from *IL-7rα^{iCre} Rosa26-YFP* mice was analyzed by flow cytometry for the indicated markers to access NK and NKT populations. Representative FACS plots of *IL-7rα^{iCre} Rosa26-YFP* mice are depicted together with YFP expression in each population in *IL-7rα^{iCre} Rosa26-YFP* mice (orange) compared to a *B6.SJL* (gray filled) control. It is noteworthy that *Tg(Vav-iCre) Rosa26-YFP* don't express the NK1.1 marker and therefore are missing in the YFP expression panel. **B.** Spleen from *IL-7rα^{iCre} Rosa26-YFP* mice was analyzed by flow cytometry for the indicated markers to acess NK and NKT populations. Representative FACS plots of *IL-7rα^{iCre} Rosa26-YFP* mice are depicted together with YFP expression in each population in *IL-7rα^{iCre} Rosa26-YFP* mice (orange) compared to a *B6.SJL* (gray filled) and a *Tg(Vav-iCre) Rosa26-YFP* (black) control. **C.** Quantification of the labeling frequencies of the NK and NKT populations in thymus and spleen. Data corresponds to 3 independent experiments, with n=3 mice in each experiment. Each dot corresponds to one mouse and the bar represents the median.

4.2. *In vivo* lineage tracing in *IL-7rα$^{iCre/+}$ Rosa26-tdTomato* mice

We analyzed *IL-7rα^{iCre} Rosa26-tdTomato* mice (Fig 4.4. A) following the same rationale as for the former mouse model: following Cre expression from the *IL-7rα^{iCre}* locus, the *Rosa26* locus is recombined and the stopper cassette excised, enabling tdTomato expression. The recombined *Rosa26-tdTomato* locus will be inherited by the cells' progeny, which will retain tdTomato expression. Negative controls were wild type *B6.SJL* mice and positive controls were *Tg(Vav-iCre) Rosa26-tdTomato* mice.

Starting the analyses in the bone marrow, we found that tdTomato was expressed in LMPP IL-7r-positive and in CLP (Fig. 4.4. B). Consistent with the former model, tdTomato was also expressed at all stages of T lymphocyte differentiation (Fig. 4.4. C). The increment in the proportion tdTomato positive thymocytes within each differentiation stage was consistent with the expression of IL-7r in those cells (Fig. 4.4. C). While the results obtained in these mice were very similar to those obtained with the YFP reporter regarding the pattern of transition from developmental stage to developmental stage, the level of cells expressing tdTomato was higher in every population (Fig. 4.4. D). This indicates that the allele *Rosa26-tdTomato* is more efficient in recombining than *Rosa26-YFP*.

Once again, the percentage of tdTomato-positive CLP was higher than that of ETP (Fig. 4.4. D). Additionally, for both LMPP and LMPP CD62L^{+} populations, the low level of tdTomato expression does not suggest an obvious direct relationship to the ETP. Nevertheless, the LMPP IL-7r^{+} had a percentage of reporter-positive cells that was similar, though lower, to that of the ETP. In this model, the difference between reporter-positive LMPP IL-7r^{+} and ETP is more obvious, which opens some questions, namely whether recombination occurs between bone marrow emigration and thymus seeding, and whether the Cre is active up until the ETP. Altogether, these data exclude the CLP as the progenitor upstream of the ETP, pointing towards LMPP IL-7r^{+} as the physiological progenitor that generates the ETP.

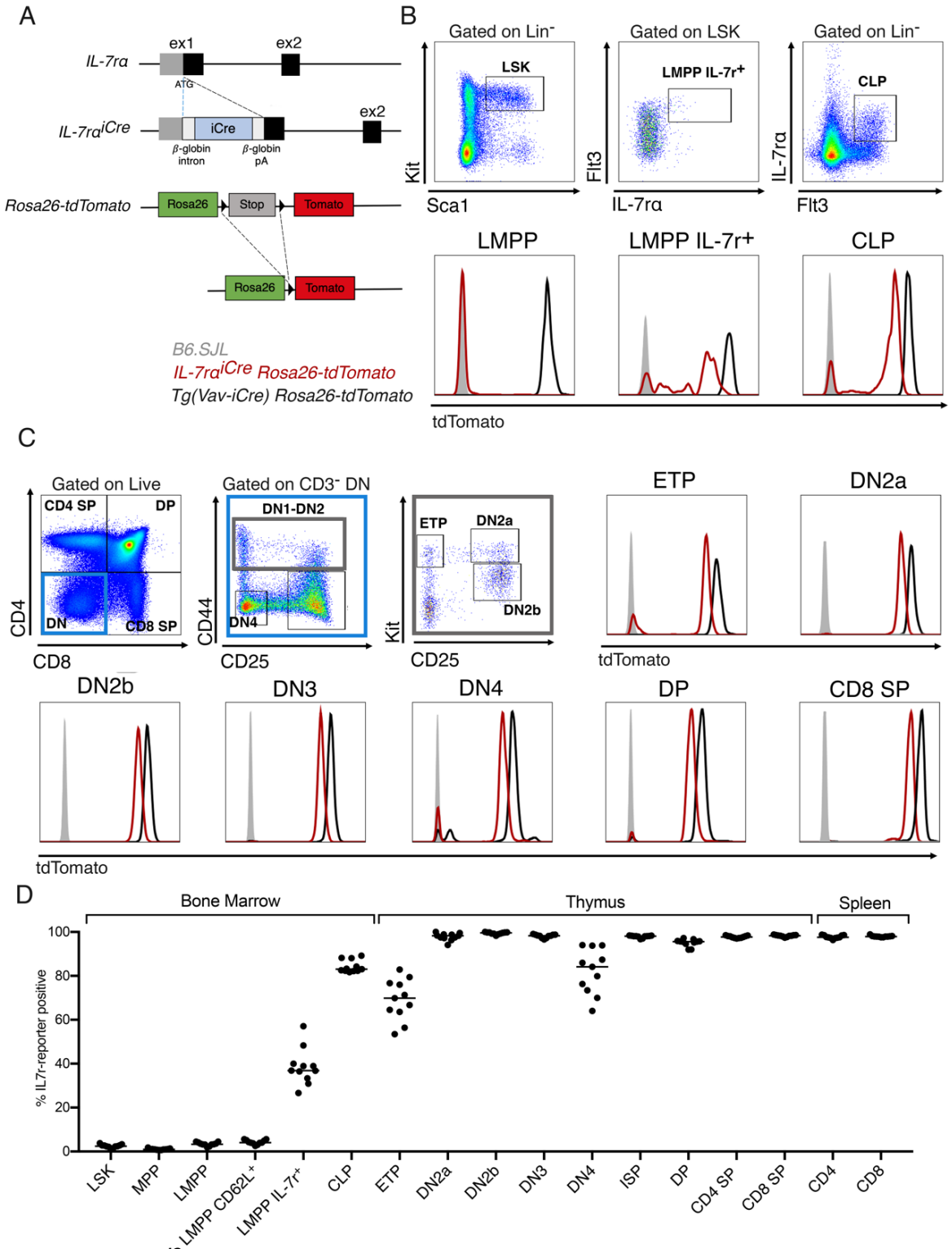

Figure 4.4. *IL-7rα^{jCre} Rosa26-tdTomato* characterization and T lymphocyte differentiation. A. Schematic representation of the wild type *IL-7rα* locus and the targeted *IL-7rα^{jCre}* allele. The *Rosa26-tdTomato* locus is represented before and after Cre mediated recombination. **B.** Bone marrow from *IL-7rα^{jCre} Rosa26-tdTomato* mice was analyzed by flow cytometry for the indicated markers to acess the candidate progenitor populations. Representative FACS plots of *IL-7rα^{jCre} Rosa26-tdTomato* mice are depicted together with tdTomato expression in each population in *IL-7rα^{jCre} Rosa26-tdTomato* mice (red) compared to a *B6.SJL* (gray filled) and a *Tg(Vav-iCre) Rosa26-tdTomato* (black) control. **C**. Thymus from *IL-7rα^{jCre} Rosa26-tdTomato* mice was analyzed by flow cytometry for the indicated markers to access T lymphocyte differentiation stages. Representative FACS plots are depicted together with tdTomato expression in each thymocyte population in *IL-7rα^{jCre} Rosa26-tdTomato* mice (red) compared to a *B6.SJL* (gray filled) and a *Tg(Vav-iCre) Rosa26-tdTomato* (black) control. **D.** Quantification of the labeling frequencies of bone marrow progenitors and thymocytes. Data corresponds to 4 independent experiments, with n=3 mice in each experiment. Each dot corresponds to one mouse and the bar represents the median.

Next, we analyzed B lymphocyte differentiation in *IL-7rα*$^{iCre/+}$ *Rosa26-tdTomato* mice (Fig. 4.5. A). We focused on the immature stages of B lymphocyte differentiation in the bone marrow and found that within B cell committed populations, 100% of the cells were tdTomato-positive (Fig. 4.5. A). The quantification of tdTomato-positive cells in the bone marrow (Fig 4.5. B) shows an increase in percentage in tdTomato-positive cells from the CLP to the pre-proB, which expresses IL-7r, compatible with the proposed progenitor-progeny relationship between these populations.

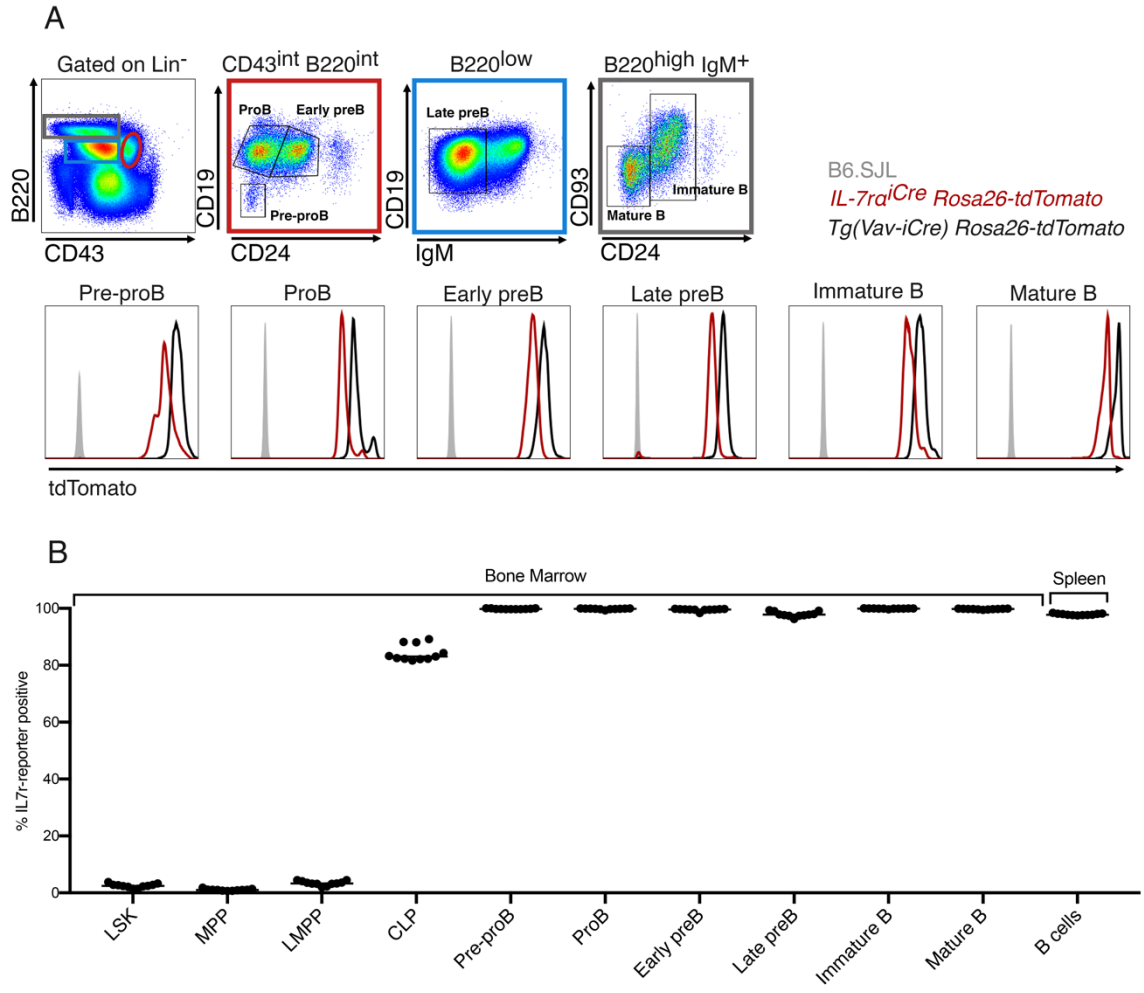

Figure 4.5. *IL-7rα*^{iCre} *Rosa26-tdTomato* mice, B lymphocyte differentiation. A. Bone marrow from *IL-7rα*^{iCre} *Rosa26-tdTomato* mice was analyzed by flow cytometry for the indicated markers to access B lymphocyte differentiation stages. Representative FACS plots of *IL-7rα*^{iCre} *Rosa26-tdTomato* mice are depicted together with tdTomato expression in each population in *IL-7rα*^{iCre} *Rosa26-tdTomato* mice (red) compared to a *B6.SJL* (gray filled) and a *Tg(Vav-iCre) Rosa26-tdTomato* (black) control. **B.** Quantification of the labeling frequencies of bone marrow progenitors and stages of B lymphocyte differentiation. Data corresponds to 4 independent experiments, with n=3 mice in each experiment. Each dot corresponds to one mouse and the bar represents the median.

NK and NKT cells in the thymus (Fig. 4.6. A) and spleen (Fig. 4.6. B) were mostly tdTomato-positive. As this model has a higher recombination than the *IL-7rα*$^{iCre/+}$ *Rosa26-YFP*, the majority of cells within these populations express the reporter. The overall quantification of tdTomato-positive cells (Fig 4.6. C) show reporter expression in all NK and NK T populations, regardless of the organ tested.

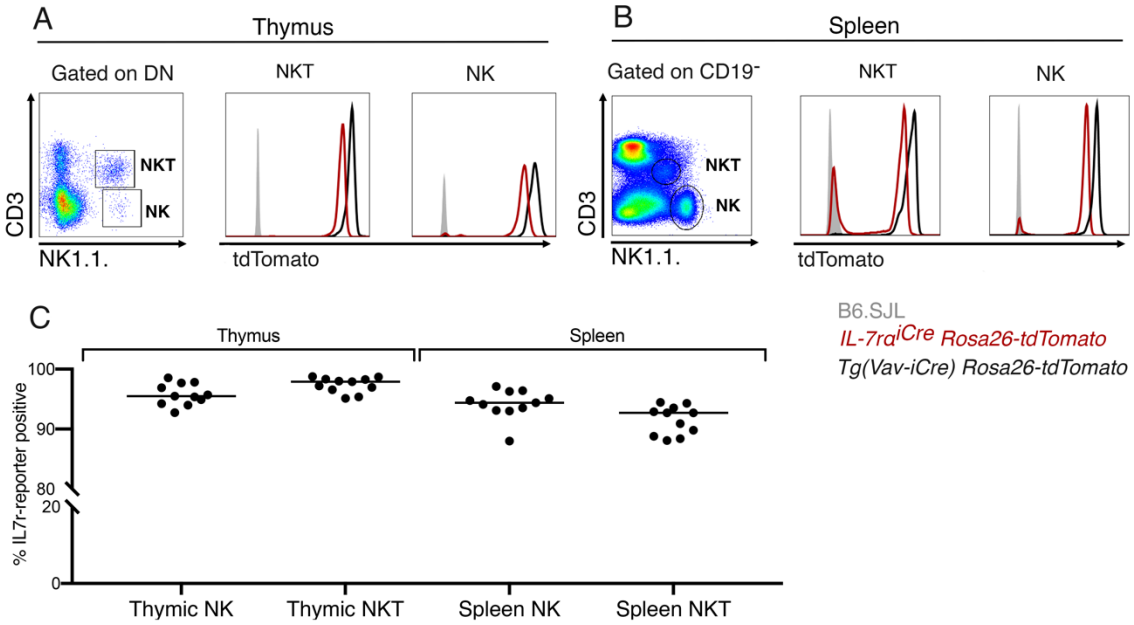

Figure 4.6. *IL-7rα*^{iCre} *Rosa26-tdTomato* mice, natural killer cells. A. Thymus from *IL-7rα*^{iCre} *Rosa26-tdTomato* mice was analyzed by flow cytometry for the indicated markers to access NK and NKT populations. Representative FACS plots of *IL-7rα*^{iCre} *Rosa26-tdTomato* mice are depicted together with tdTomato expression in each population in *IL-7rα*^{iCre} *Rosa26-tdTomato* mice (red) compared to a *B6.SJL* (gray filled) and a *Tg(Vav-iCre) Rosa26-tdTomato* (black) control. **B.** Spleen from *IL-7rα*^{iCre} *Rosa26-tdTomato* mice was analyzed by flow cytometry for the indicated markers to acess NK and NKT populations. Representative FACS plots of *IL-7rα*^{iCre} *Rosa26-tdTomato* mice are depicted together with tdTomato expression in each population in *IL-7rα*^{iCre} *Rosa26-tdTomato* mice (red) compared to a *B6.SJL* (gray filled) and a *Tg(Vav-iCre) Rosa26-tdTomato* (black) control. **C.** Quantification of the labeling frequencies of the NK and NKT populations in the thymus and in the spleen. Data corresponds to 4 independent experiments, with n=3 mice in each experiment. Each dot corresponds to one mouse and the bar represents the median.

As a means to assess the specificity of the model, we also analyzed reporter expression in myeloid lineages, as most do not express IL-7r during their differentiation, and therefore should also lack reporter expression in *IL-7rα*$^{iCre/+}$ *Rosa26-tdTomato* mice. We focused on the spleen and analyzed eosinophils, neutrophils, dendritic cells and macrophages (Fig 4.7. A). As predicted, most myeloid populations were reporter-negative (Fig 4.7. B). The exception was a small subset of dendritic cells that was reporter-positive, most likely to correspond to plasmacytoid dendritic cells that express IL-7r (46) (Fig 4.7. B). Finally, we detected that 5% of splenic macrophages also expressed tdTomato (Fig. 4.7. B). This was surprising and we consider that this might be explained by phagocytosis of dead or dying cells that

express the reporter (47,48). Nevertheless, further studies would be required to clarify if that is indeed the case.

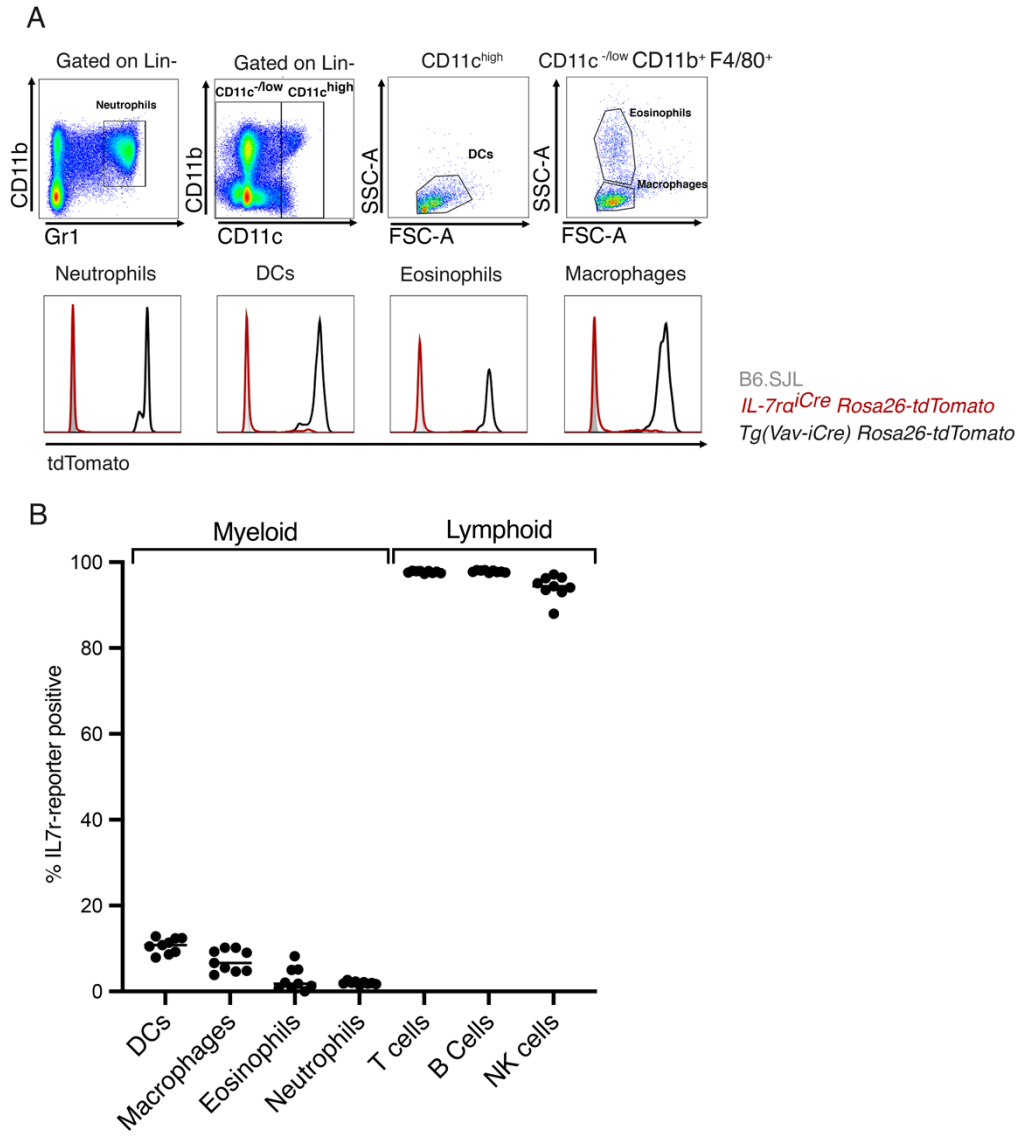

Figure 4.7. *IL-7rα^{jCre} Rosa26-tdTomato* mice, myeloid lineages. A. Spleen from *IL-7rα^{jCre} Rosa26-tdTomato* mice was analyzed by flow cytometry for the indicated markers to acess myeloid populations. Representative FACS plots of *IL-7rα^{jCre} Rosa26-tdTomato* mice are depicted together with tdTomato expression in each population in *IL-7rα^{jCre} Rosa26-tdTomato* mice (red) compared to a *B6.SJL* (gray filled) and a *Tg(Vav-iCre) Rosa26-tdTomato* (black) control. **B.** Quantification of the labeling frequencies of myeloid and lymphoid populations in the spleen. Data corresponds to 3 independent experiments, with n=3 mice in each experiment. Each dot corresponds to one mouse and the bar represents the median.

4.3. Testing LMPP and CLP subsets for T lymphocyte potential *in vivo*

If LMPP IL-7r+ is indeed the direct progenitor of the T lymphocytes, then its potential should be higher when compared to other progenitors. In order to test which of four potential candidate progenitors was better at generating T lymphocytes *in vivo,* we performed adoptive transfers into *IL-7rα*$^{-/-}$ recipients. These recipient mice have open thymic niches and therefore allow for efficient reconstitution of the thymus without the need of previous irradiation (35,49). The different progenitors were isolated and sort-purified from the bone marrow of *B6.SJL* wild type mice. Recipient and donor cells were distinguished with basis on the differential expression of CD45.1 (donor) and CD45.2 (host).

Sorted populations CLP Ly6D^{-}, CLP Ly6D^{+}, LMPP IL-7r^{+} and LMPP IL-7r^{-} (Fig. 4.8. A) were injected i.v. and thymi were analyzed 21 days after reconstitution (Fig. 4.8. B). Each recipient mouse received either 1500 LMPP IL-7r^{+} cells, 1500 LMPP IL-7r^{-}, 7865 CLP Ly6D^{+} or 7865 CLP Ly6D^{-}. The time point of analysis was chosen to detect the peak of double positive thymocytes generated from the injected progenitors. Although both LMPP IL-7r^{-} and LMPP IL-7r^{+} generated thymocytes (Fig 4.8. C), the efficiency was much higher for the LMPP IL-7r+ (Fig. 4.8. D). As for CLP, while CLP Ly6D^{-} generated thymocytes, CLP Ly6D^{+} failed to do so (Fig. 4.8. C and D). The latter population has been described to be primed towards the B lymphocyte lineage (32) and the result is therefore not surprising. Nevertheless, even with ~5-fold less LMPP IL-7r^{+} (1500 cells) as compared to CLP Ly6D^{-} (7865 cells), IL-7r^{+} LMPP generated more double positive thymocytes (Fig. 4.8. D).

The number of sorted CLP vs LMPP differed for technical reasons. Therefore, to compare the T lymphocyte potential of the different progenitors, we calculated the number of double positive thymocytes generated per cell injected. Then, the differences became even more evident, as each LMPP IL-7r^{+} injected generated ~10 000 double positive cells, while each CLP Ly6D^{-} generated ~1000 (Fig. 4.8. D). Altogether, these data suggest that the LMPP IL-7r^{+} has the highest T lymphocyte potential among the tested populations.

We also analyzed the spleen for the presence of B lymphocytes that differentiated from the injected progenitors to control for our injection (Fig. 4.8. E). All mice had B lymphocytes in the spleen, confirming that the measured results in the thymus were indeed specific and not due to technical differences in injection.

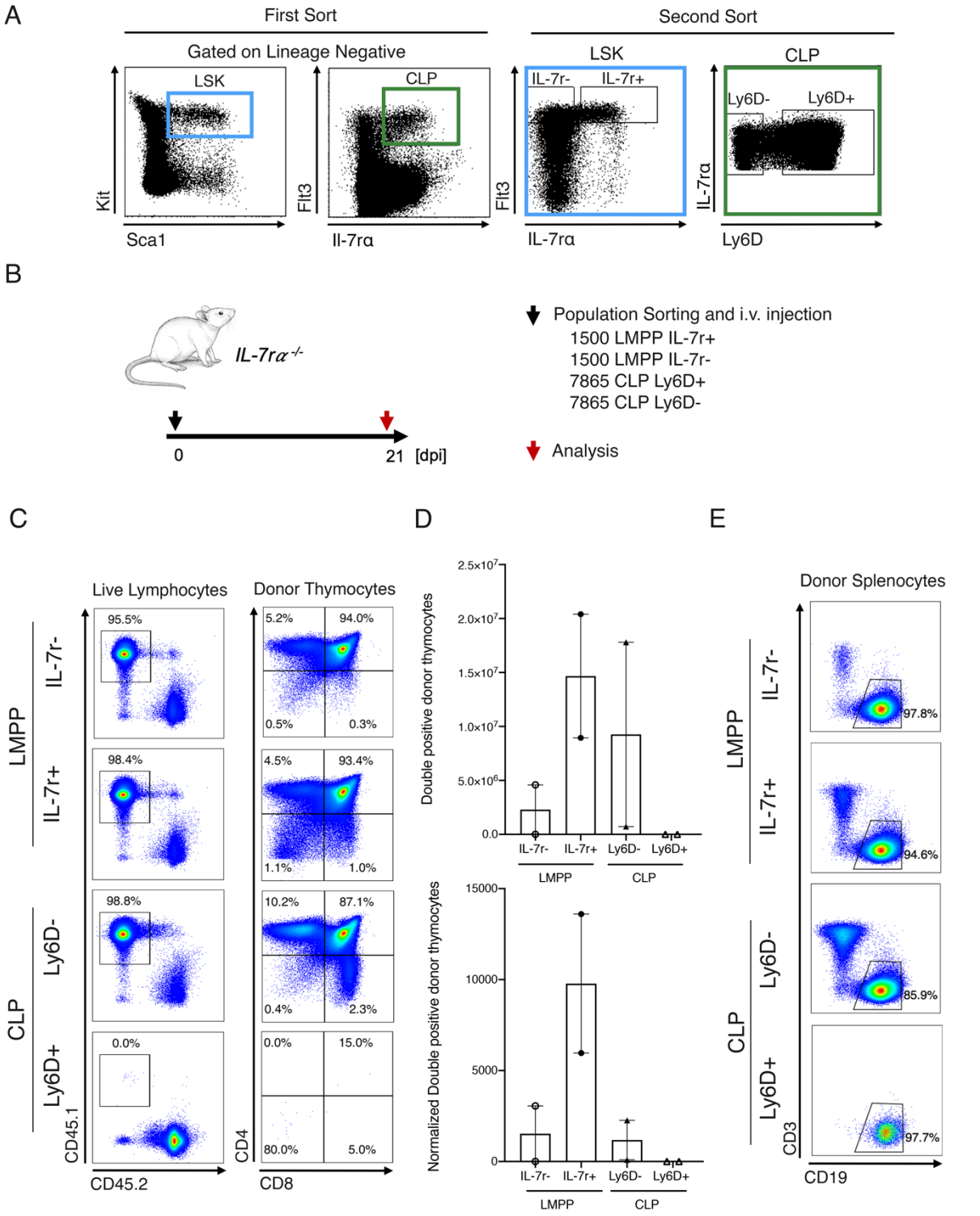

Figure 4.8. Adoptive transfers into *IL-7rα*$^{-/-}$ mice. A. LSK (Lineage-negative, Sca1-positive, Kit-positive) and CLP (Lineage-negative, IL-7r-positive, Flt3-positive) were sorted from *B6.SJL* (CD45.1) mice. Afterwards, previously sorted LSK were further sorted into LMPP IL-7r^{+} and LMPP IL-7r^{-}. Sorted CLP were further sorted into CLP Ly6D^{+} and CLP Ly6D^{-}. **B.** *IL-7rα*$^{-/-}$ Recipient mice (CD45.2) were injected intravenously (i.v.) with the sorted populations. From the LMPP IL-7r^{+} and IL-7r^{-}, 1500 cells were injected into the recipients. From the CLP Ly6D^{+} and Ly6D^{-}, 7865 cells were injected. Reconstituted recipient mice were analysed 21 days after reconstitution. **C.** Thymus from recipient mice was analyzed by flow cytometry for the indicated markers to acess donor (CD45.1-positive) double positive thymocytes. Representative FACS plots of each experiental group of mice are depicted. **D.** Quantification of double positive donor thymocytes and normalized data (normalized number of donor double positive thymocytes per cell injected). Each dot corresponds to one mouse, bars represent the median with 95% confidence interval. **E**. Spleen from recipient mice was analyzed by flow cytometry for the indicated markers to acess donor (CD45.1-positive) B lymphocytes. Representative FACS plots of each experiental group of mice are depicted.

Finally, we compared the proportion of reporter-positive cells within each of these bone marrow populations to the proportion of reporter-positive ETP. Total CLP as well as Ly6D-negative CLP and Ly6D-positive CLP had a higher proportion of reporter-positive cells than that of the ETP (Fig. 4.9.). This suggests that the CLP as a whole is unlikely to be the direct progenitor of the ETP population. LMPP IL-7r^{+} had a slightly lower proportion of reporter-positive cells than the ETP, favoring the hypothesis that LMPP IL-7r^{+} could be upstream of the T cell lineage.

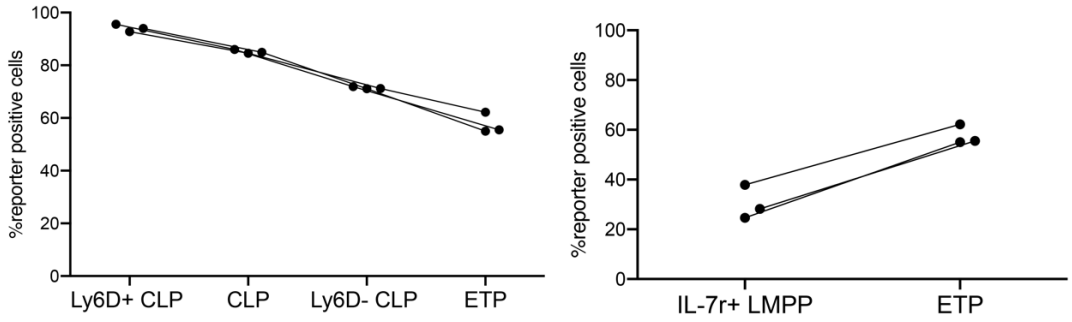

Figure 4.9. Labeling frequencies in bone marrow progenitors and ETP. Quantification of the labeling frequencies of bone marrow progenitors and ETP in *IL-7rα^{iCre} Rosa26-tdTomato* mice. Data corresponds to 1 independent experiment, with n=3 mice. Lines connect populations in the same mouse.

4.4. Inducible lineage tracing in *IL-7rα$^{iCreERT2/+}$ Rosa26-YFP* mice

The previous results support LMPP IL-7r^{+} as the most likely progenitor in the bone marrow that gives rise to the T lymphocyte lineage. Next, we sought to understand the dynamics of hematopoietic progenitor egress from the bone marrow and seeding into the thymus in unperturbed, physiological conditions. For that purpose, an inducible system of induction of Cre recombinase activity was developed in the lab. Specifically, *IL-7rα$^{iCreERT2/+}$* mice were generated by targeting the *IL-7rα* endogenous locus and inserting the coding sequence for *iCre-ERT2* (Fig. 4.10. A) following a strategy similar to the one used for the previously described mice. Then the mice were crossed to obtain *IL-7rα$^{iCreERT2/+}$ Rosa26-YFP* mice (Fig. 4.10. A). In this model, iCre-ERT2 is expressed in an inactive form that is activated upon tamoxifen injection (50). These mice were injected intraperitoneally (i.p.) with tamoxifen for five consecutive days, following the protocol used by others (51), and analyzed one day after the last injection (Fig. 4.10. B). Non-injected littermates *IL-7rα$^{iCreERT2/+}$ Rosa26-YFP* mice were used as negative controls. The quantification of YFP-positive cells in the bone marrow and the thymus shows that after 5 injections of tamoxifen, the levels of recombination were very low (Fig. 4.10. C). Moreover, the tamoxifen administration caused a significant reduction in thymus cellularity, with most populations decreased (Fig. 4.10. D), which could be either due to the delivery system employed (i.p. injection) or the tamoxifen dosage which could trigger Cre or tamoxifen-toxicity (52,53). As the recombination efficiency was too low to be possible to interpret results, we decided not to pursue this mouse model further.

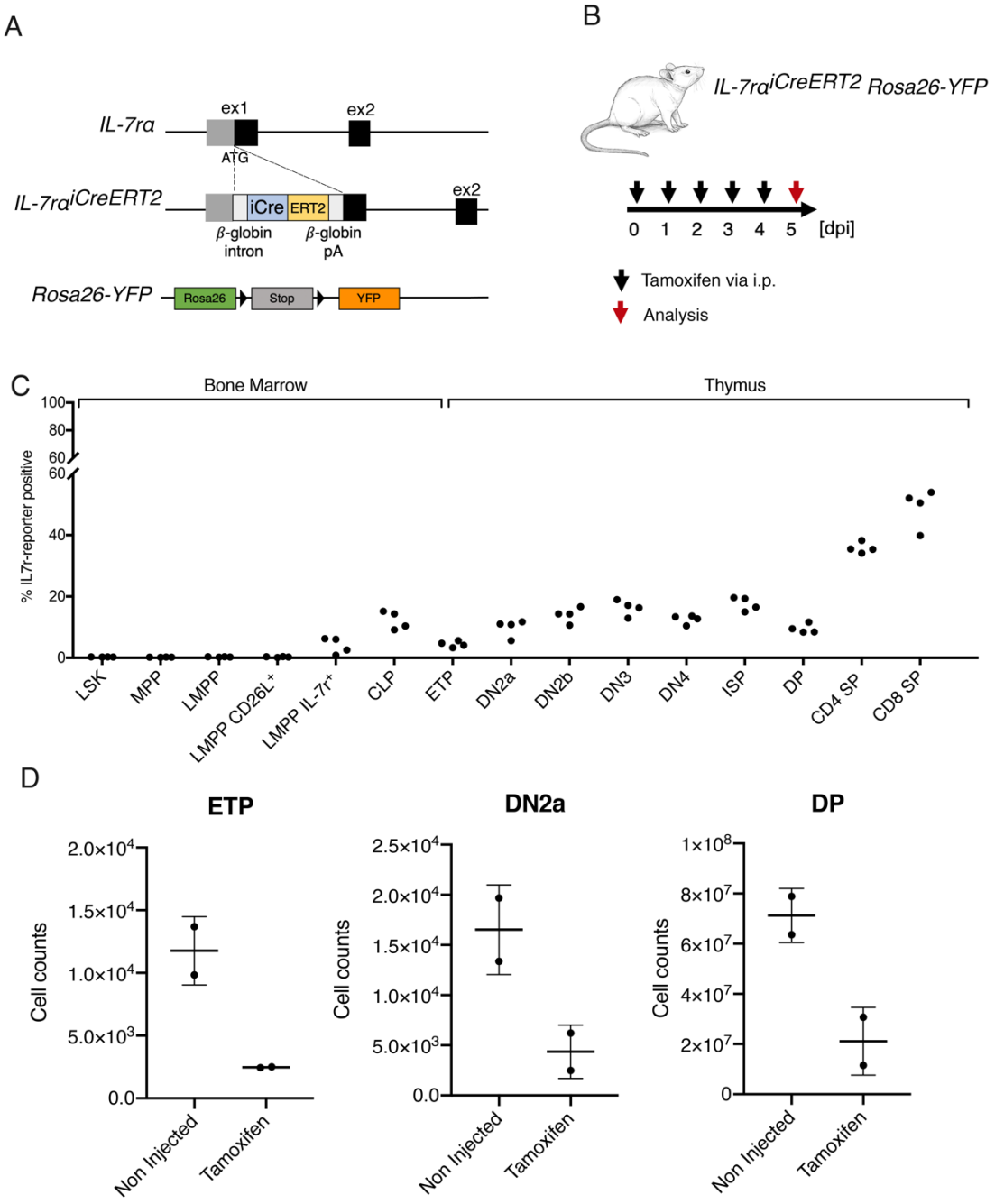

Figure 4.10. *IL-7rα*$^{jCreERT2/+}$ *Rosa26-YFP* mice. A. Schematic representation of the wild type *IL-7rα* locus and the targeted *IL-7rα*^{jCreERT2} allele. The *Rosa26-YFP* locus is represented before Cre mediated recombination. **B.** *IL-7rα*$^{jCreERT2/+}$ *Rosa26-YFP* mice were injected 5 consecutive days with 1 mg tamoxifen via intraperitoneal (i.p.) injection. Mice were analyzed 5 days post first injection (dpi). **C.** Quantification of the labelling frequencies of bone marrow progenitors and thymocytes after 5 injection of tamoxifen, 5 consecutive days. Data corresponds to one experiment, with n=4 mice. Each dot corresponds to one mouse. **D.** Quantification of early T cell precursors (ETP), DN2a and double positive (DP) populations in control littermate mice and in mice after 5 injections of tamoxifen. Data corresponds to one experiment, with n=2 mice in each experimental condition. Each dot corresponds to one mouse, and the bars represent the median with 95% confidence interval.

4.5. Inducible lineage tracing in *IL-7rα$^{iCreERT2/+}$ Rosa26-tdTomato* mice

Following the inefficiency of induced recombination with the previous mouse model, we focused on *IL-7rα^{iCreERT2} Rosa26-tdTomato* mice (Fig. 4.11. A) and tested the best protocol of tamoxifen induction to label cells with the least secondary effects possible (Fig. 4.11. B). We tested 3 protocols: 1) 5 daily consecutive doses via gavage, 2) one single dose of tamoxifen via gavage, and 3) one single dose injected interperitoneally (i.p.). Mice were analyzed 1 day after the last injection (Fig. 4.11. B), and non-injected littermates were used as negative controls. When comparing the levels of recombination between protocols 1 and 2 (Fig. 4.11. C) we found that although 5 doses induced higher recombination, this was associated with a strong effect in reducing cellularity (Fig. 4.11. E). Furthermore, one single dose of tamoxifen was sufficient to enable recombination in several populations (Fig. 4.11. D), and the levels of recombination were compatible with different levels of IL-7r expression in different populations. Although this test was done only once, tamoxifen delivery via gavage seemed to be more consistent (Fig. 4.11. D). Therefore, all following experiments were done using one single dose of tamoxifen, delivered via gavage.

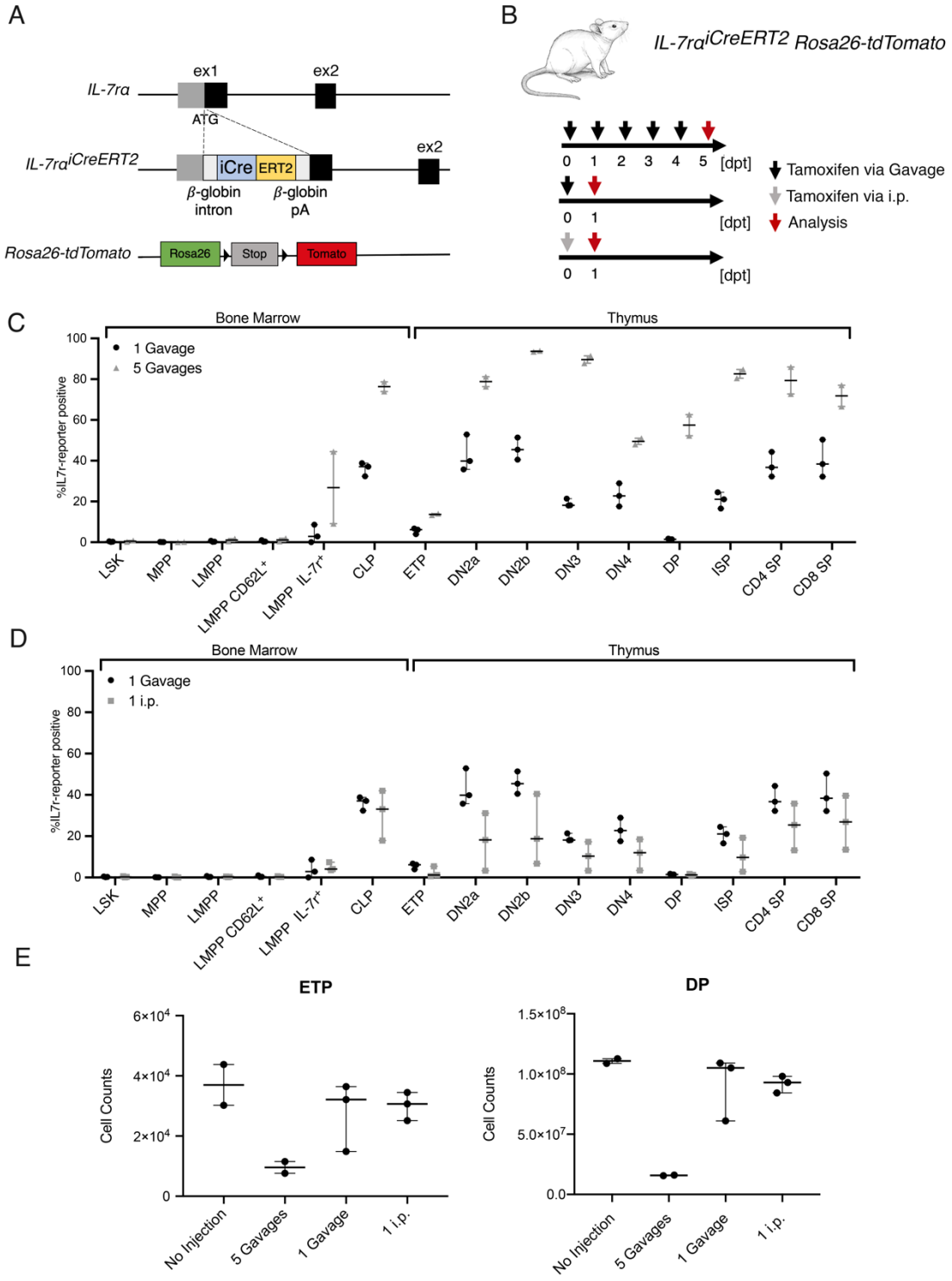

Figure 4.11. Selection of the best protocol for tamoxifen-induced recombination in *IL-7rα$^{jCreERT2/+}$ Rosa26-tdTomato* mice. A. Schematic representation of the wild type *IL-7rα* locus and the targeted *IL-7rα^{jCreERT2} allele. The Rosa26-tdTomato* locus is represented before Cre mediated recombination ***B.*** *IL-7rα$^{jCreERT2/+}$ Rosa26-tdTomato* mice were submitted to 5-daily administration of tamoxifen via gavage (protocol 1) or 1 mg of tamoxifen via gavage or via intraperitoneal (i.p.) injection (Protocol 2 and 3, respectively). Mice were analyzed 1- or 5-days post tamoxifen (dpt) administration. **C.** Quantification of the labelling frequencies of bone marrow progenitors and thymocytes after 1 or 5 doses of tamoxifen via gavage. Data corresponds to 1 experiment, with n=3 mice in 1 dose condition and n=2 in 5 doses condition**. D.** Quantification of the labelling frequencies of bone marrow progenitors and thymocytes after 1 dose of tamoxifen via gavage or via i.p. Data corresponds to 1 experiment, with n=3 mice in each experimental protocol. **E.** Quantification of early T cell precursor (ETP) and double positive (DP) populations in control littermate mice and in mice after submitted to one of the 3 protocols described in B. Each dot corresponds to one mouse, and the bars represent the median with 95% confidence interval.

With the best protocol in hand, we analyzed *IL-7rα$^{iCreERT2/+}$ Rosa26-tdTomato* mice at different timepoints after tamoxifen administration (Fig. 4.12. A). In this system, we specifically labeled IL-7r-expressing cells, and then followed their progression in the relevant bone marrow and thymic populations. As T lymphocyte differentiation is very well studied, we started by analyzing the thymus to validate the mouse model. All populations analyzed, from the DN2 through DN3 to DN4 started expressing tdTomato following tamoxifen administration and reached maximum levels of labeling 2 days later (Fig 4.12. B). From then on, the percentage of labeled cells started to decrease (Fig. 4.12. B). This shows that tamoxifen is available for a maximum of two days, during which recombination of the *Rosa26* locus takes place, marking those cells that expressed the *Cre-ERT2* from the *IL-7rα* locus. Afterwards, each marked cell compartment will differentiate further and loose the marked cells. Increase in reporter-positive cells in any cell compartment can therefore only be explained by incoming cells that differentiated from a previous cell compartment that was labeled at higher levels. This becomes obvious in the next stages of differentiation, if one focuses from the DN4, to the immature single positive (ISP), to double positive, and finally the CD4 or CD8 single positive thymocytes (Fig. 4.12. C). Double positive thymocytes express barely any IL-7r and therefore do not become labelled in the first days after tamoxifen administration. This happens only later in time due to differentiation from the earliest cell compartments (Fig. 4.12. C), consistent with reports that the transition from DN4 to ISP and DP is very fast, taking about 2/3 days (4,21). Although essentially no double positive cells were labeled 2 days after tamoxifen administration, by 10 days, they presented a robust proportion of labeled cells that only declined thereafter (Fig. 4.12. C). This is compatible with the reported differentiation time of approximately 7-10 days from DN2/DN3 to DP (4,21). Taken together, these data demonstrated that progenitor-progeny relationships could be accurately defined for the thymus based on our mouse model, supporting that we could move to the next step of addressing progenitor-progeny relationships between the bone marrow and the thymus.

Focusing on the main bone marrow progenitors studied before, the CLP and the LMPP IL-7r^{+}, we quantified the percentage of reporter-positive cells and compared them with the earliest stages of differentiation in the thymus (Fig. 4.12. D). Both CLP and the LMPP IL-7r^{+} were labeled within 2 days consistent with IL-7r expression. Afterwards, both CLP and LMPP IL-7r^{+} lose reporter-positive cells, as they differentiate and are replaced by non-marked cells. We expected that the maximum level of reporter-positive ETP would recapitulate that of its direct counterpart in the bone marrow, although at a later timepoint. Although our prediction was that the ETP would mirror the LMPP IL-7r^{+} with some delay, that was not the case. Instead, ETP reached 23% labeling efficiency by day 7. This was surprising and further experiments will be required to clarify these data and help us interpret these results.

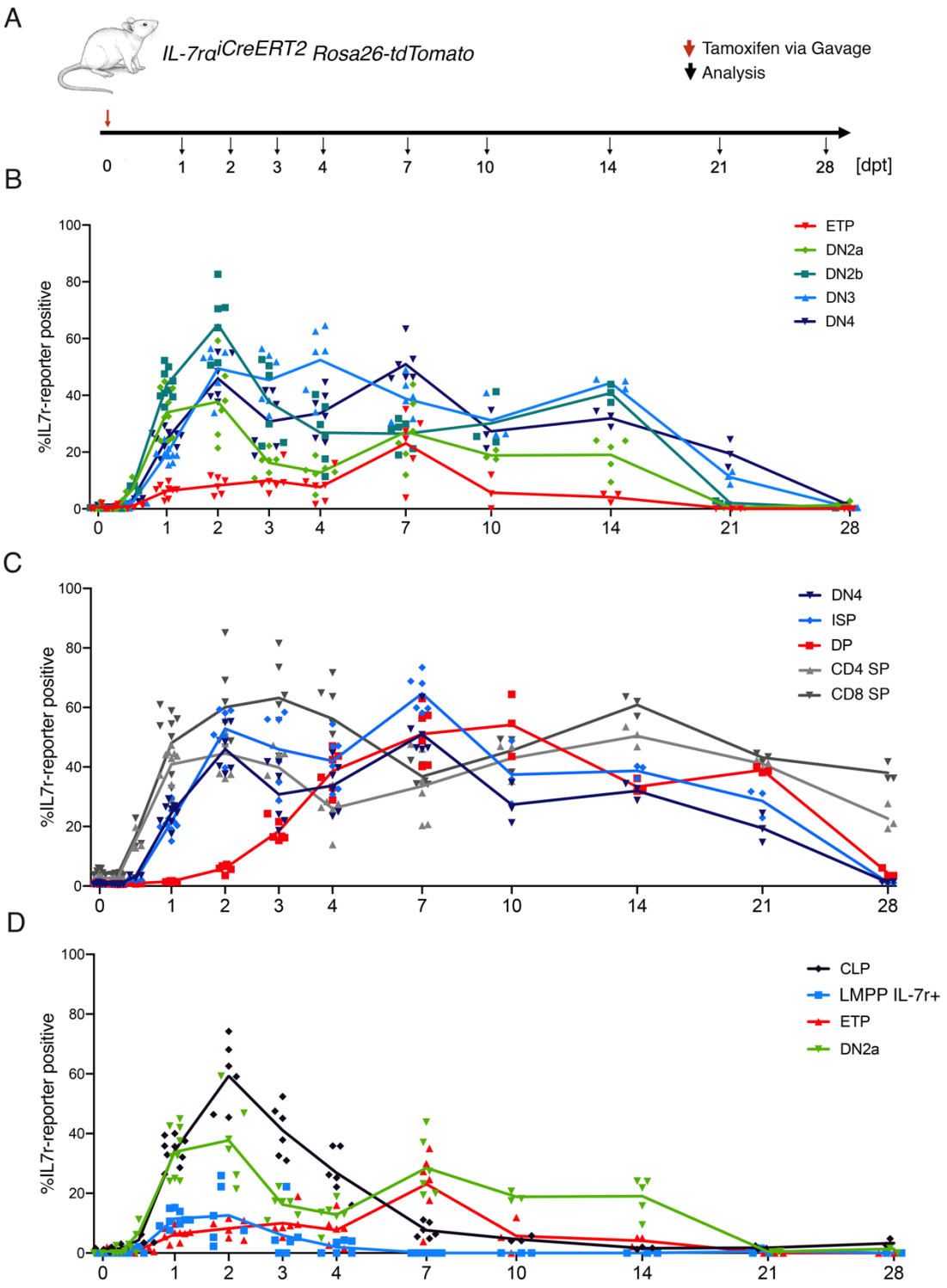

Figure 4.12. **Thymocyte kinetics with the *IL-7rα*$^{iCreERT2/+}$ *Rosa26-tdTomato* mice. A.** Mice received one tamoxigen administration via gavage and were analysed at several timepoints thereafter. Diferent cohort of mice were analysed at diferent timepoints. Mice were analized 6 and 12 hours after gavage and also several days post tamoxifen (dpt) adminstration. **B.** Quantification of the labeling frequencies of ETP, DN2a, DN2b, DN3 and DN4 ploted over time after one tamoxifen gavage. Lines connecting all timepoins were ploted to better visualise the kynetics of each population. Lines connect medians of each timepoint for each population. **C.** Quantification of the labeling frequencies of DN4, ISP, DP, CD4 SP and CD8 SP ploted over time after one tamoxifen gavage. Lines connecting all timepoins were ploted to better visualise the kynetics of each population. Lines connect medians of each timepoint for each population. **D.** Quantification of the labeling frequencies of the two here proposed bone marrow progenitors and thymocyte populations ETP and DN2a ploted over time after one tamoxifen gavage. Lines connecting all timepoins were ploted to better visualise the kynetics of each population. Lines connect medians of each timepoint for each population.

4.6. Comparing CLP Ly6D$^-$ and LMPP IL-7r$^+$

CLP were originally described as Lineage-negative, IL-7r-positive, Kit-low and Sca1-low (25), and subsequently refined for Flt3 expression (31). Further studies have refined the current strategy to gate CLP, which consists in selecting lineage-negative, Flt3-positive, IL-7r-positive cells (Fig. 4.13. A). Nevertheless, CLP are recognized as a heterogeneous population, and the subdivision based on Ly6D enables to discriminate between B lymphocyte restricted (Ly6D-positive) and non-restricted (Ly6D-negative) CLP (Fig. 4.13. A) (32). Interestingly, Ly6D-negative CLP present higher levels of Kit and Sca1, compared to the Ly6D-positive fraction, where Kit expression is practically absent. This means that there might be some overlap between Ly6D-negative CLP and LMPP IL-7r$^+$ (Fig. 4.13. B).

Within LMPP, L-selectin (CD62L) has been used to mark a subpopulation proposed to be the progenitor of the T lymphocyte lineage, following the rationale that L-selectin is required for thymus seeding (33,54). Interestingly, the majority of LMPP IL-7r$^+$ express L-selectin and is hence included in the LMPP L-selectin population (Fig. 4.13. B). If we gate the cells is the opposite way, we can see that LMPP IL-7r+ are in fact a minority within the LMPP L-selectin (Fig. 4.13. B).

At this stage we do not have a black and white picture that enables us to point with certainty at one population in the bone marrow and tell that this is the direct progenitor upstream of the T lymphocyte lineage, but further work will clarify our current knowledge.

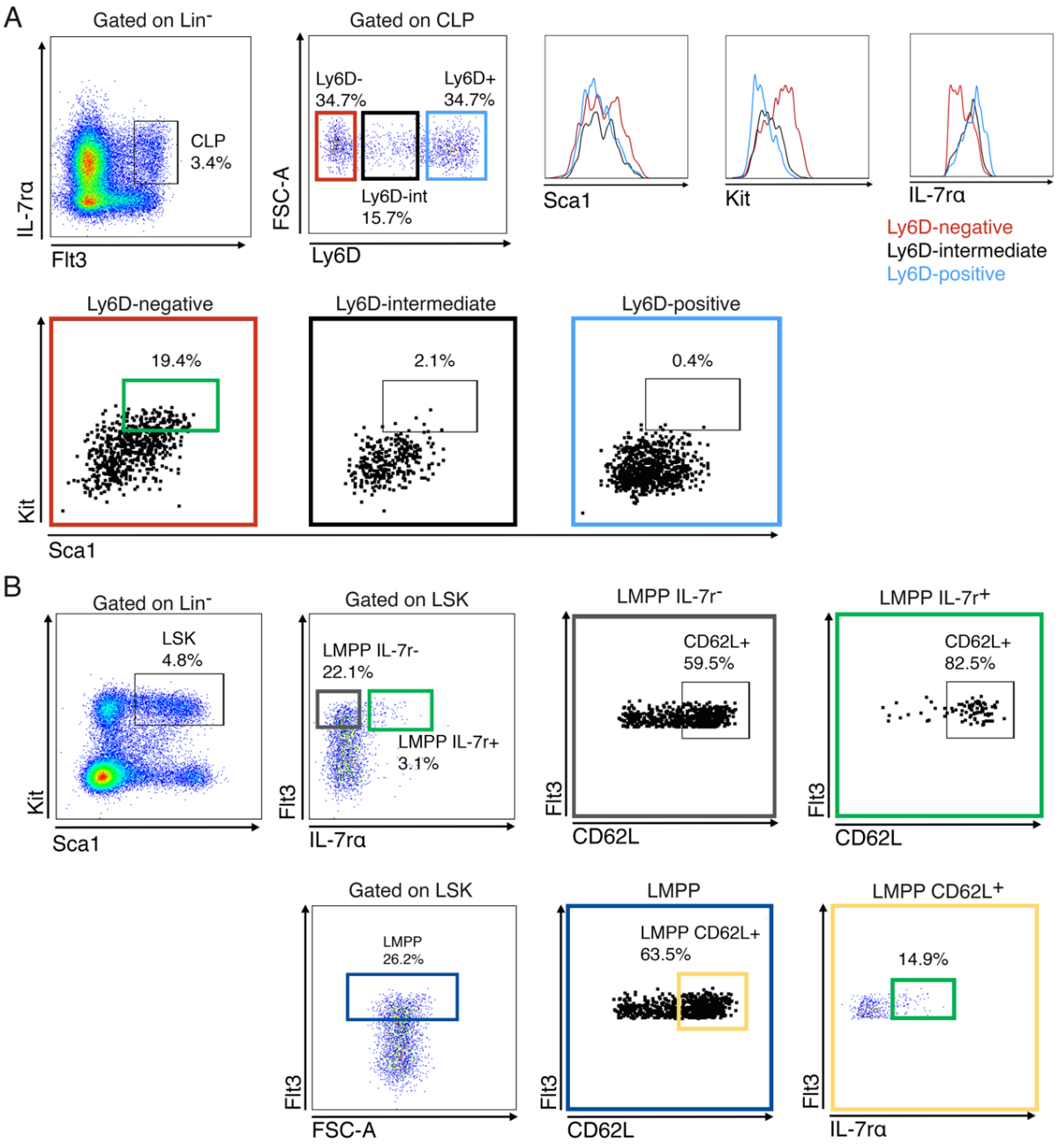

Figure 4.13. Progenitor characterization. A. Bone marrow from *B6.SJL* mice was analyzed by flow cytometry for the indicated markers to acess CLP heterogeneity. Representative FACS plots of *B6.SJL* mice are depicted and Ly6D-negative (red), intermediate (black) and positive (blue) CLP were plotted to acess Kit versus Sca1 profile. Histograms of Kit, Sca1 and IL-7r expression are also depicted in each of the CLP subpopulations. **B.** Bone marrow from *B6.SJL* mice was analyzed by flow cytometry for the indicated markers to acess LMPP heterogeneity. Representative FACS plots representing LMPP (dark blue), LMPP IL-7r^{+} (green), LMPP IL-7r^{-} (dark grey) and LMPP CD62L^{+} (yellow) are depicted. The green rectangle identifies the overlapping LMPP IL-7r^{+} population.

5. Discussion

Most hematopoietic lineages differentiate in the bone marrow. T lymphocytes are the exception by differentiating in an anatomically distinct organ, the thymus. As the progenitors that generate T lymphocytes originate in the bone marrow, they must migrate into the thymus, and their identity has been a focus of research, with several candidates suggested. In this dissertation, we addressed this question using *in vivo* lineage tracing and adoptive transfer experiments in mice. We generated mouse models that allowed us to trace progenitor-progeny relationships in lymphopoiesis: *IL-7rα^{iCre} Rosa26-YFP* and *IL-7rα^{iCre} Rosa26-tdTomato*. The pattern of reporter-positive cells throughout T and B lymphocyte differentiation was similar between both mouse models. However, the values of reporter-positive cells were substantially higher in the latter, consistent with higher efficiency of recombination of the *Rosa26-tdTomato* allele. These mice permitted the identification of a population of hematopoietic progenitors in the bone marrow that is consistent with a progenitor-progeny relationship giving rise to the thymic ETP. The data were supported by adoptive transfer experiments into recipients described to have open thymic niches (49).

The design of *IL-7rα^{iCre}* followed a previously published design (41). However, while that report showed that both CLP an ETP were ~80% reporter-positive (41), the same populations in our mice were recombined at consistently lower values. Furthermore, the percentage of reporter-positive CLP were well above those of reporter-positive ETP, which can only be explained if the recombination in our mice is much less efficient and, importantly, the CLP (as a whole) cannot be the bone marrow counterpart of the thymic ETP. The reasons for the discrepancy between our results and those already published (41) is unclear. The recombination efficiency is clearly lower in our hands even with the same reporter (*Rosa26-YFP*) that was used in the former study (41). While our aim was to obtain the same design, the targeting strategy was different: we first generated an *IL-7rα^{iCreERT2}* mouse line by CRISPR-Cas9 technology in 1 cell-stage embryos, afterwards, we used the line for a second gene targeting for removal of the ERT2 sequence. Current work in our lab proceeds to characterize the targeted locus, which has the expected configuration 5' followed by the complete coding sequence for *iCre*. However, the 3' end of the gene differs from the expected, and results are consistent with a Cre recombinase that has an additional random sequence fused downstream, that might reduce protein stability or activity.

Although unexpected, the reduced efficiency of the reporter was advantageous, as by enabling lower recombination efficiency, it increased resolution within and between the populations of interest. In this regard, even the choice of reporter makes the difference: although the *IL-7rα^{iCre} Rosa26-tdTomato* had a better recombination efficacy, the lower proportion of reporter-positive cells in *IL-7rα^{iCre} Rosa26-YFP* offered better resolution in detailing both B and T lymphocyte differentiation. We consider very likely that the recombination was close to saturation in the original publication (41), while in our case not all cells expressing the *IL-7rα* locus will recombine the *Rosa26* locus.

In both mouse models, reporter-positive ETP are compatible with the fact that they develop from an IL-7r expressing progenitor because IL-7r expression in ETP is low to undetectable by FACS. Therefore, the assumption is that the percentage of reporter-positive cells represent a history of IL-7r expression rather than active expression of the gene, and this ought to reflect the percentage of reporter-positive progenitors upstream of the ETP. Although the CLP has been pointed as the most likely progenitor of the ETP (41), our data challenges that view. Instead, we found that there are LMPP that express IL-7r (LMPP IL-7r^{+}), which are composed of a percentage of reporter-positive cells that is more similar to the ETP. Nevertheless, if we plot these cells to determine the degree of overlap between LMPP IL-7r^{+} and CLP, we can see that there is some overlap, with LMPP IL-7r^{+} falling within the CLP gate, and vice versa. Taken together, our data supports LMPP IL-7r^{+} as the physiological progenitors of T lymphocytes, although it remains to be tested whether there is a significant overlap between progenitor populations.

Seeking to learn about the dynamics of bone marrow emigration to thymus seeding, we analyzed *IL-7rα^{iCreERT2} Rosa26-tdTomato* mice, and induced reporter recombination transiently. We found that following induction, populations that express IL-7r reach a maximum of reporter-positive cells within 2 days, and continuously decrease thereafter. This indicates that tamoxifen is bioavailable for at most two days, enabling the recombination of the reporter locus. Thereafter, turnover replaces reporter-positive cells by reporter-negative cells. Cell populations with increasing percentage of reporter-positive cells after two days are due to cellular input from former stages with higher percentage of reporter-positive cells. This dynamic enable determining the kinetics between differentiation stages, that were in accordance with the literature, validating the system to focus on our questions. Unexpectedly, ETP were labeled immediately and reached 10% reporter-expression by 2-day post induction. This can only be explained if some ETP express IL-7r, or if bone marrow progenitors seed the thymus to contribute to this percentage within 2 days following tamoxifen administration. ETP label remains constant afterwards, and peaks by day 7 with 23% of the ETPs labeled. If the sole factor regulating the proportion of recombined cells at ETP were the input from progenitor cells from the bone marrow, one would expect that there would be an exact match between the proportion of reporter-positive progenitor cells and reporter-positive ETP at some stage in time. With this is mind, it is not easy to conciliate our results obtained with the inducible model and the former, obtained with the constitutively expressed Cre, that pointed at the LMPP IL-7r^{+} as the direct progenitor of the ETP. At this stage, rather than a closed story, we have additional questions that are still unanswered. Are we missing the right cell population in the bone marrow? We will need to expand our analyses to cover for additional timepoints and additional markers in the bone marrow, including the possibility that IL-7r-positive cells proliferate more than their IL-7r-negative counterparts at some stage.

6. Conclusion and future remarks

Altogether the data validated both constitutive *IL-7rα^{iCre} Rosa26-YFP* and *IL-7rα^{iCre} Rosa26-tdTomato* models as useful tools for *in vivo* study of lymphopoiesis in an unperturbed system. Combined data from non-manipulated *in vivo* lineage tracing mice and adoptive transfers support the LMPP IL-7r^{+} population as the refined progenitor to the thymus seeding progenitor rather than CLP. Interestingly, LMPP IL-7r^{+} has some overlap with CLP and express high levels of L-selectin, a molecule involved in thymus seeding. In addition, inducible *IL-7rα^{iCreERT2} Rosa26-tdTomato* mice closely recapitulates the kinetics of thymocyte differentiation and therefore was validated as a powerful tool to study the kinetics of bone marrow export and thymus import. However, further work will be necessary to clarify the apparent incompatibility of results between the constitutive vs. inducible models. Additional timepoints will be required in the latter model to better define progenitor kinetics. Also, it will be important to test whether progenitors that recombine the reporter locus have a higher expression of IL-7r and whether these might have a proliferative advantage. Future work could comprise *in vitro* studies to better characterize the potential of the candidate thymus seeding progenitors to generate T lymphocytes. To this purpose, progenitors would be co-cultured with bone marrow-derived stromal cell line (OP9) ectopically expressing the Notch ligand Delta-like 4 (Dll4) to stimulate T lymphocyte development. Moreover, RNAseq analysis must be performed to compare the transcriptomic profiles between these progenitors and the most immature thymocytes. In sum, this project allowed us to gain knowledge that integrates the interaction between the bone marrow and the thymus and allowed us to clarify the identity of the progenitor that emigrates out of the bone marrow and seeds the thymus to support T lymphocyte differentiation.

Bibliography

1. Murphy K, Weaver C. Janeway's Immunobiology. 9th ed. Garland Science, editor. Garland Science, New York. 2017.
2. Abbas A, Lichtman AH, Pillai S. Cellular and Molecular Immunology 9th Ed. Cellular and Molecular Immunology. 2017.
3. Bianchi ME. DAMPs, PAMPs and alarmins: all we need to know about danger. J Leukoc Biol. 2007;
4. Paul WE. Fundamental Immunology. 7th Ed. Lippincott Williams & Wilkins, editor. 2013.
5. Manz MG, Traver D, Miyamoto T, Weissman IL, Akashi K. Dendritic cell potentials of early lymphoid and myeloid progenitors. Blood. 2001;
6. Scimone ML, Aifantis I, Apostolou I, Von Boehmer H, Von Andrian UH. A multistep adhesion cascade for lymphoid progenitor cell homing to the thymus. Proc Natl Acad Sci U S A. 2006;
7. Wang LD, Clark MR. B-cell antigen-receptor signalling in lymphocyte development. Immunology. 2003.
8. Reth M. Antigen receptors on B lymphocytes. Annual Review of Immunology. 1992.
9. Vyas JM, Van Der Veen AG, Ploegh HL. The known unknowns of antigen processing and presentation. Nature Reviews Immunology. 2008.
10. Neefjes J, Jongsma MLM, Paul P, Bakke O. Towards a systems understanding of MHC class i and MHC class II antigen presentation. Nature Reviews Immunology. 2011.
11. Busslinger M. Transcriptional control of early B cell development. Annual Review of Immunology. 2004.
12. Medvedovic J, Ebert A, Tagoh H, Busslinger M. Pax5: A Master Regulator of B Cell Development and Leukemogenesis. In: Advances in Immunology. 2011.
13. Kikuchi K, Kasai H, Watanabe A, Lai AY, Kondo M. IL-7 Specifies B Cell Fate at the Common Lymphoid Progenitor to Pre-ProB Transition Stage by Maintaining Early B Cell Factor Expression. J Immunol. 2008;
14. Clark MR, Mandal M, Ochiai K, Singh H. Orchestrating B cell lymphopoiesis through interplay of IL-7 receptor and pre-B cell receptor signalling. Nature Reviews Immunology. 2014.
15. Enver T. B-cell commitment: Pax5 is the deciding factor. Current Biology. 1999.
16. Min H, Montecino-Rodriguez E, Dorshkind K. Effects of Aging on the Common Lymphoid Progenitor to Pro-B Cell Transition. J Immunol. 2006;
17. Hardy RR, Carmack CE, Shinton SA, Kemp JD, Hayakawa K. Resolution and characterization of pro-B and pre-pro-B cell stages in normal mouse bone marrow. J Exp Med. 1991;
18. Hardy RR, Kincade PW, Dorshkind K. The Protean Nature of Cells in the B Lymphocyte Lineage. Immunity. 2007.
19. Petrenko O, Beavis A, Klaine M, Kittappa R, Godin I, Lemischka IR. The molecular characterization of the fetal stem cell marker AA4. Immunity. 1999;
20. Shlomchik MJ, Weisel F. Germinal center selection and the development of memory B and plasma cells. Immunol Rev. 2012;
21. Krueger A, Ziętara N, Łyszkiewicz M. T Cell Development by the Numbers. Trends in Immunology. 2017.
22. Petrie HT. Cell migration and the control of post-natal T-cell lymphopoiesis in the thymus. Nature Reviews Immunology. 2003.
23. Goldrath AW, Bevan MJ. Selecting and maintaining a diverse T-cell repertoire. Nature. 1999.
24. Workman CJ, Szymczak-Workman AL, Collison LW, Pillai MR, Vignali DAA. The development and function of regulatory T cells. Cellular and Molecular Life Sciences. 2009.
25. Kondo M, Weissman IL, Akashi K. Identification of clonogenic common lymphoid progenitors in mouse bone marrow. Cell. 1997;
26. Bhandoola A, von Boehmer H, Petrie HT, Zúñiga-Pflücker JC. Commitment and Developmental Potential of Extrathymic and Intrathymic T Cell Precursors: Plenty to Choose from. Immunity. 2007.
27. Zietara N, Łyszkiewicz M, Puchałka J, Witzlau K, Reinhardt A, Förster R, et al. Multicongenic fate mapping quantification of dynamics of thymus colonization. J Exp Med. 2015;
28. Ceredig R. Fates and potentials of thymus-seeding progenitors. Nature Immunology. 2012.
29. Saran N, Łyszkiewicz M, Pommerencke J, Witzlau K, Vakilzadeh R, Ballmaier M, et al. Multiple extrathymic precursors contribute to T-cell development with different kinetics. Blood. 2010;
30. Adolfsson J, Månsson R, Buza-Vidas N, Hultquist A, Liuba K, Jensen CT, et al. Identification of Flt3+ lympho-myeloid stem cells lacking erythro-megakaryocytic potential: A revised road map for adult blood lineage commitment. Cell. 2005;

31. Karsunky H, Inlay MA, Serwold T, Bhattacharya D, Weissman IL. Flk2 + common lymphoid progenitors possess equivalent differentiation potential for the B and T lineages. Blood. 2008;
32. Inlay MA, Bhattacharya D, Sahoo D, Serwold T, Seita J, Karsunky H, et al. Ly6d marks the earliest stage of B-cell specification and identifies the branchpoint between B-cell and T-cell development. Genes Dev. 2009;
33. Perry SS, Wang H, Pierce LJ, Yang AM, Tsai S, Spangrude GJ. L-selectin defines a bone marrow analog to the thymic early T-lineage progenitor. Blood. 2004;
34. Luc S, Luis TC, Boukarabila H, Macaulay IC, Buza-Vidas N, Bouriez-Jones T, et al. The earliest thymic T cell progenitors sustain B cell and myeloid lineage potential. Nat Immunol. 2012;
35. Peschon JJ, Morrissey PJ, Grabstein KH, Ramsdell FJ, Maraskovsky E, Gliniak BC, et al. Early Lymphocyte Expansion Is Severely Impaired in Interleukin 7 Receptor-deficient Mice. J Exp Med. 1994;
36. Madisen L, Zwingman TA, Sunkin SM, Oh SW, Zariwala HA, Gu H, et al. A robust and high-throughput Cre reporting and characterization system for the whole mouse brain. Nat Neurosci. 2010;
37. Srinivas S, Watanabe T, Lin CS, William CM, Tanabe Y, Jessell TM, et al. Cre reporter strains produced by targeted insertion of EYFP and ECFP into the ROSA26 locus. BMC Dev Biol. 2001;
38. de Boer J, Williams A, Skavdis G, Harker N, Coles M, Tolaini M, et al. Transgenic mice with hematopoietic and lymphoid specific expression of Cre. European Journal of Immunology. 2003.
39. Shimshek DR, Kim J, Hübner MR, Spergel DJ, Buchholz F, Casanova E, et al. Codon-improved Cre recombinase (iCre) expression in the mouse. Genesis. 2002;
40. Casanova E, Fehsenfeld S, Lemberger T, Shimshek DR, Sprengel R, Mantamadiotis T. ER-based double iCre fusion protein allows partial recombination in forebrain. Genesis. 2002;
41. Schlenner SM, Madan V, Busch K, Tietz A, Läufle C, Costa C, et al. Fate Mapping Reveals Separate Origins of T Cells and Myeloid Lineages in the Thymus. Immunity. 2010;
42. Hong C, Luckey MA, Park JH. Intrathymic IL-7: The where, when, and why of IL-7 signaling during T cell development. Seminars in Immunology. 2012.
43. Bonanni V, Sciumè G, Santoni A, Bernardini G. Bone marrow NK cells: Origin, distinctive features, and requirements for tissue localization. Frontiers in Immunology. 2019.
44. Vosshenrich CAJ, García-Ojeda ME, Samson-Villéger SI, Pasqualetto V, Enault L, Goff OR Le, et al. A thymic pathway of mouse natural killer cell development characterized by expression of GATA-3 and CD127. Nat Immunol. 2006;
45. de Lalla C, Festuccia N, Albrecht I, Chang H-D, Andolfi G, Benninghoff U, et al. Innate-Like Effector Differentiation of Human Invariant NKT Cells Driven by IL-7. J Immunol. 2008;
46. Guimond M, Veenstra RG, Grindler DJ, Zhang H, Cui Y, Murphy RD, et al. Interleukin 7 signaling in dendritic cells regulates the homeostatic proliferation and niche size of CD4+ T cells. Nat Immunol. 2009;
47. Mcgaha TL, Karlsson MCI. Apoptotic cell responses in the splenic marginal zone: A paradigm for immunologic reactions to apoptotic antigens with implications for autoimmunity. Immunol Rev. 2016;
48. Gordon S, Plüddemann A. Macrophage clearance of apoptotic cells: A critical assessment. Frontiers in Immunology. 2018.
49. Prockop SE, Petrie HT. Regulation of Thymus Size by Competition for Stromal Niches among Early T Cell Progenitors. J Immunol. 2004;
50. Indra AK, Warot X, Brocard J, Bornert JM, Xiao JH, Chambon P, et al. Temporally-controlled site-specific mutagenesis in the basal layer of the epidermis: Comparison of the recombinase activity of the tamoxifen-inducible Cre-ER(T) and Cre-ER(T2) recombinases. Nucleic Acids Res. 1999;
51. Busch K, Klapproth K, Barile M, Flossdorf M, Holland-Letz T, Schlenner SM, et al. Fundamental properties of unperturbed haematopoiesis from stem cells in vivo. Nature. 2015;
52. Loonstra A, Vooijs M, Beverloo HB, Allak B Al, Van Drunen E, Kanaar R, et al. Growth inhibition and DNA damage induced by Cre recombinase in mammalian cells. Proc Natl Acad Sci U S A. 2001;
53. Bohin N, Carlson EA, Samuelson LC. Genome Toxicity and Impaired Stem Cell Function after Conditional Activation of CreER T2 in the Intestine. Stem Cell Reports. 2018;
54. Schwarz BA, Sambandam A, Maillard I, Harman BC, Love PE, Bhandoola A. Selective Thymus Settling Regulated by Cytokine and Chemokine Receptors. J Immunol. 2007;